

1 **Growth of the coccolithophore *Emiliana huxleyi* in light- and nutrient-limited batch**
2 **reactors: relevance for the BIOSOPE deep ecological niche of coccolithophores**

3
4 **Laura Perrin¹, Ian Probert², Gerald Langer³ and Giovanni Aloisi⁴**

5 ¹Sorbonne Universités, UPMC Univ. Paris 06 -CNRS-IRD-MNHN, LOCEAN-IPSL, 75252 Paris, France.

6 ²CNRS-UPMC Univ. Paris 06 FR2424, Roscoff Culture Collection, Station Biologique de Roscoff, 29680 Roscoff, France.

7 ³The Marine Biological Association of the United Kingdom, The Laboratory, Citadel Hill, Plymouth, Devon, PL1 2PB, UK.

8 ⁴LOCEAN, UMR 7159, CNRS-UPMC-IRD-MNHN, 75252 Paris, France.

9
10 Correspondence to: L. Perrin (lpelod@locean-ipsl.upmc.fr)

11
12 Abstract. Coccolithophores are unicellular calcifying marine algae that play an important role in the oceanic
13 oceanic carbon cycle via their cellular processes of photosynthesis (a CO₂ sink) and calcification (a CO₂
14 source). In contrast to the well-studied, shallow-water coccolithophore blooms visible from satellites, the
15 lower photic zone is a poorly known but potentially important ecological niche for coccolithophores in
16 terms of primary production and carbon export to the deep ocean. In this study, the physiological
17 responses of an *Emiliana huxleyi* strain to conditions simulating the deep niche in the oligotrophic gyres
18 along the BIOSOPE transect in the South Pacific oceanic gyre were investigated. We carried out batch
19 culture experiments with an *E. huxleyi* strain isolated from the BIOSOPE transect, reproducing the in situ
20 conditions of light- and nutrient- (nitrate and phosphate) limitation. By simulating coccolithophore growth
21 using an internal stores (Droop) model, we were able to constrain fundamental physiological parameters
22 for this *E. huxleyi* strain. We show that simple batch experiments, in conjunction with physiological
23 modelling, can provide reliable estimates of fundamental physiological parameters for *E. huxleyi* that are
24 usually obtained experimentally in more time-consuming and costly chemostat experiments. The
25 combination of culture experiments, physiological modelling and in situ data from the BIOSOPE cruise
26 shows that *E. huxleyi* growth in the deep BIOSOPE niche is co-limited by availability of light and nitrate. This
27 study contributes more widely to the understanding of *E. huxleyi* physiology and behavior in a low-light and
28 oligotrophic environment of the ocean.

29 **Keywords**

30 Coccolithophores, batch cultures, deep niche, South Pacific Gyre, Droop model, physiological parameters.

36 1. Introduction

37 Coccolithophores are unicellular photosynthetic and calcifying algae that are very abundant in the
38 marine environment and play key roles in the global carbon cycle (Paasche, 2002; Roth, 1994). Through
39 photosynthesis they contribute to the upper ocean carbon pump (CO₂ sink), while via calcification they
40 contribute to the carbonate counter-pump (CO₂ source) (Paasche, 2002; Westbroek et al., 1993). The
41 relative importance of calcification and photosynthesis is one of the factors that dictates the effect of
42 coccolithophores on ocean-atmosphere CO₂ fluxes (Shutler et al., 2013). Environmental conditions such as
43 temperature, irradiance, nutrient concentrations and pCO₂ exert a primary control on the
44 calcification/photosynthesis ratio in coccolithophores and also affect cellular growth rates, which, together
45 with grazing, mortality, sinking of cells and oceanic transport, define the biogeography of coccolithophores.
46 Despite the fact that certain coccolithophores have been fairly extensively studied in the laboratory (e.g.
47 Daniels et al., 2014; Iglesias-Rodriguez et al., 2008; Krug et al., 2011; Langer et al., 2012; Rouco et al., 2013),
48 the factors controlling their biogeography in the global ocean are poorly understood (Boyd et al., 2010). In
49 controlled laboratory conditions, coccolithophore growth is monitored as given environmental parameters
50 are varied (e.g. Buitenhuis et al., 2008; Feng et al., 2008; Fritz, 1999; Langer et al., 2006; Leonardos and
51 Geider, 2005; Paasche, 1999; Trimborn et al., 2007). In the ocean, geographical surveys of coccolithophore
52 abundance and concomitant measurements of environmental variables contribute to defining
53 coccolithophore biogeography in relation to the environment (Claustre et al., 2008; Henderiks et al., 2012).
54 Although extrapolation of results from laboratory experiments to field distributions might not be
55 straightforward, this approach has been widely used and continues to yield important insights into
56 coccolithophore ecology and their reactions to a rapidly changing environment.

57
58 In this respect, one of the least well understood, but possibly globally relevant niches where
59 coccolithophores can be relatively abundant is that occurring at the deep pycnocline of oceanic gyres,
60 probably the best studied example of which was observed during the BIOSOPE cruise in the South Pacific
61 Gyre (Beaufort et al., 2008; Claustre et al., 2008). This deep coccolithophore niche occurred at about 200 m
62 depth, at a very low irradiance level ($< 20 \mu\text{mol photons m}^{-2} \text{s}^{-1}$) and at a depth corresponding to the nitrate
63 and phosphate nutricline with dissolved nitrate (NO₃) and phosphate (PO₄) concentrations of about 1 μM
64 and 0.2 μM , respectively. The niche was dominated by coccolithophore species belonging to the family
65 Noëlaerhabdaceae, i.e. *Emiliania huxleyi* and species of *Gephyrocapsa* and *Reticulofenestra* (Beaufort et al.,
66 2008). Deep-dwelling coccolithophores have also been observed in other geographic regions. Okada and
67 McIntyre (1979) observed coccolithophores in the North Atlantic Ocean down to a depth of 100 m where
68 *Florisphaera profunda* dominated assemblages in summer and *E. huxleyi* for the rest of the year. Deep
69 coccolithophore populations dominated by *F. profunda* in the lower photic zone (LPZ > 100 m) of
70 subtropical gyres were observed by Cortés et al. (2001) in the Central North Pacific Gyre (station ALOHA)

71 and by Haidar and Thierstein (2001) in the Sargasso Sea (North Atlantic Ocean). Jordan and Winter (2000)
72 reported assemblages of coccolithophores dominated by *F. profunda* in the LPZ in the north-east Caribbean
73 with a high abundance and co-dominance of *E. huxleyi* and *G. oceanica* through the water column down to
74 the top of the LPZ. These deep-dwelling coccolithophores are not recorded by satellite-based remote
75 sensing methods (Henderiks et al., 2012; Winter et al., 2014) that detect back-scattered light from
76 coccoliths from a layer only a few tens of meters thick at the surface of the ocean (Holligan et al., 1993;
77 Loisel et al., 2006).

78
79 Understanding the development of deep coccolithophore populations in low nutrient, low irradiance
80 environments would contribute to building a global picture of coccolithophore ecology and biogeography.
81 Laboratory culture experiments with coccolithophores that combine both nutrient and light limitation,
82 however, are scarce. One reason is that investigating phytoplankton growth under nutrient limitation in
83 laboratory experiments is complicated. In batch cultures the instantaneous growth rate decreases as
84 nutrients become limiting, making it hard to extract the dependence of growth rate on nutrient
85 concentrations (Langer et al., 2013). This can be avoided by employing chemostat cultures, in which growth
86 rates and nutrient concentrations are kept constant under nutrient-limited conditions (Engel et al., 2014;
87 Leonardos and Geider, 2005; Müller et al., 2012). Physiological parameters obtained in chemostat
88 experiments have been used in biogeochemical models to investigate environmental controls on
89 phytoplankton biogeography (Follows and Dutkiewicz, 2011; Gregg and Casey, 2007). Despite their
90 relevance to nutrient limited growth, chemostat cultures are relatively rarely used because they are more
91 expensive, time-consuming and complicated to set up and run than batch cultures (LaRoche et al., 2010).

92
93 In this study, we investigated growth of the coccolithophore *E. huxleyi* under light and nutrient co-
94 limitation and applied the results of this culture study to investigate the conditions controlling growth in
95 the deep niche of the South Pacific Gyre. Using an *E. huxleyi* strain isolated during the BIOSOPE cruise, we
96 carried out batch culture experiments that reproduced the low in situ light and nutrient conditions of the
97 deep ecological niche. We monitored the nitrogen and phosphorus content of particulate organic matter,
98 as well as cell, coccosphere and coccolith sizes, because these parameters are known to vary with nutrient
99 limitation (Fritz, 1999; Kaffes, 2010; Rouco et al., 2013). To overcome the conceptual limitations inherent in
100 nutrient-limited batch experiments (Langer et al., 2013), we modeled the transient growth conditions in the
101 batch reactor assuming that assimilation of nutrients and growth are either coupled (Monod, 1949) or
102 decoupled (Droop, 1968) processes in the coccolithophore *E. huxleyi*. An independent check of our
103 modelling approach was obtained by also modeling the *E. huxleyi* batch culture data of Langer et al. (2013).
104 The range of physiological parameters that can be directly assessed in batch culture experiments is limited
105 (Eppley et al., 1969; Marañón et al., 2013). We show that batch cultures, if coupled to simple physiological
106 modeling, may provide valuable estimates of fundamental physiological parameters that are more widely

107 obtained in more time-consuming and costly chemostat experiments (Eppley and Renger, 1974; Terry,
108 1982; Riegman et al., 2000; Müller et al., 2012). Our joint culture and modelling approach also provides
109 information on the conditions that control the growth of *E. huxleyi* in the deep ecological niche of the South
110 Pacific Gyre.

111

112 **2. Materials and methods**

113 **2.1 Experimental**

114 **2.1.1 Growth medium and culture conditions**

115 Natural seawater collected near the Roscoff Biological Station (Brittany, France) was sterile-filtered
116 and enhanced to K (-Si,-Tris, +Ni, -Cu) medium according to Keller et al. (1987), with only nitrate (no
117 ammonium) as a nitrogen source. *Emiliana huxleyi* strain RCC911, isolated in summer 2004 from a water
118 sample collected at 10 m depth near the Marquesas Islands during the BIOSOPE cruise (November to
119 December 2004), was grown in batch cultures. Experiments were conducted in triplicate in 2.7 litre
120 polycarbonate bottles (Nalgene) with no head space. Experimental conditions were chosen to reproduce
121 those prevalent in surface waters and at the nitricline of the oligotrophic gyre in the South Pacific Ocean
122 (Morel et al., 2007). Cultures were grown under a 12:12 hour light:dark (L:D) cycle (taken from a calculation
123 of L:D cycle at the GYR station at the date of the sampling), at a temperature of 20°C and at a salinity of
124 34.7. Cultures were grown at two irradiance levels: high light (ca. 140 $\mu\text{mol photons m}^{-2} \text{s}^{-1}$) and low light
125 (ca. 30 $\mu\text{mol photons m}^{-2} \text{s}^{-1}$). The latter corresponds to the upper end of the irradiance range of the deep
126 BIOSOPE coccolithophore niche (10-30 $\mu\text{mol photons m}^{-2} \text{s}^{-1}$). We chose not to run experiments at
127 irradiance levels lower than 30 $\mu\text{mol photons m}^{-2} \text{s}^{-1}$ in order to avoid very long experimental runs. Nutrient
128 concentrations at the beginning of batch experiments were 100 μM and 2.5-5.1 μM for nitrate and 6.25
129 and 0.45-0.55 μM for phosphate in nutrient-replete and nutrient-limited conditions, respectively. For each
130 irradiance level, three experiments were carried out (in triplicate): control (nutrient-replete), phosphate
131 limited (P-limited) and nitrate limited (N-limited) conditions. Cells were acclimated to light, temperature
132 and nutrient conditions for at least three growth cycles prior to experiments.

133 **2.1.2 Cell enumeration and growth rate**

134 The growth of batch cultures was followed by conducting cell counts every day or every other day
135 using a BDFacs Canto II flow cytometer. Experiments were stopped before the cell density reached ca.
136 $1.5 \cdot 10^5 \text{ cells mL}^{-1}$ in order to minimize shifts in the dissolved inorganic carbon (DIC) system. Cultures
137 remained in the exponential growth phase throughout the duration of the control (nutrient-replete)
138 experiments. In these control cultures, the growth rate (μ) was obtained by conducting a linear regression
139 of the cell density data on the logarithmic scale. Nutrient-limited experiments were allowed to run until
140 growth stopped. The growth rate in nutrient limited conditions decreases in time as nutrients are depleted
141 and it is therefore not possible to calculate growth rate by means of regression analysis (Langer et al.,

142 2013). The dependence of growth rate on nutrient concentration in nutrient-limited conditions was
143 investigated with the numerical model introduced in Sect. 2.2 below.

144 **2.1.3 Cell and coccosphere diameter and coccolith length**

145 Samples were taken at the end of the experiments at roughly the same point in the L:D cycle (between
146 noon and 4pm) to acquire images of cells using an optical microscope (x100, oil immersion, Olympus BX51
147 microscope). The internal cell diameter of 100 cells was measured for each experimental culture using the
148 ImageJ software (<http://rsbweb.nih.gov/ij/>). Images of coccospheres and coccoliths were obtained with
149 scanning electron microscopy (SEM). For SEM observations, samples were filtered onto 0.8 μm
150 polycarbonate filters (Millipore), rinsed with a basic solution (180 μL of 25 % ammonia solution in 1 litre of
151 MilliQ water) and dried at 55°C for 1 h. After mounting on an aluminum stub, they were coated with gold-
152 palladium and images were taken with a Phenom G2 pro desktop scanning electron microscope. For each
153 experimental culture 100 coccospheres were measured using ImageJ. Three hundred coccoliths per sample
154 were measured using a script (Young et al., 2014) that is compatible with ImageJ in order to measure the
155 distal shield length (DSL) of coccoliths.

156 **2.1.4 Dissolved inorganic carbon (DIC) and nutrient analyses**

157 Subsamples for pH_T (pH on the total scale), DIC and nutrient analyses were taken from culture media
158 at the beginning and at the end of each experiment. The pH was measured with a pHmeter-potentiometer
159 pHenomenal pH1000L with a Ross ultra combination pH electrode on the total scale (precision ± 0.02 pH
160 units) and was calibrated with a TRIS buffer. Samples for the determination of DIC were filtered through
161 pre-combusted (4 h at 450°C) glass-fibre filters (Whatman GF/F) into acid-washed glass bottles and
162 poisoned with mercuric chloride. Bottles were stored at 4°C prior to analysis. A LICOR7000 $\text{CO}_2/\text{H}_2\text{O}$ gas
163 analyzer was used for DIC analysis (precision $\pm 2 \mu\text{mol kg}^{-1}$). A culture aliquot (100 mL) was filtered onto
164 pre-combusted (4 h at 450°C) glass-fibre filters (Whatman GF/F) and stored at -20°C in a polyethylene flask
165 until nutrient analysis. Nitrate and phosphate concentrations were measured using an auto analyzer Seal
166 Analytical AA3 (detection limits were 0.003 μM for PO_4 and 0.01 μM for NO_3).

167 **2.1.5 POC, PON, PIC, POP**

168 For particulate organic carbon (POC), particulate organic nitrogen (PON), and particulate organic
169 phosphorus (POP) analyses, samples (200 or 250 mL) were filtered onto pre-combusted (4 h at 450°C) glass-
170 fibre filters (Whatman GF/F) and preserved at -20°C. POC and PON were measured on the same filter that
171 was dried overnight at 50°C after being placed in a fuming hydrochloric acid dessicator for 2 h to remove
172 coccolith calcite. POC and PON were analyzed using a NC Analyzer Flash EA 1112. Particulate inorganic
173 carbon (PIC) was obtained by using a 7500cx Agilent ICP-MS to analyze the calcium concentration in
174 samples filtered onto 0.8 μm polycarbonate filters (Millipore) and extracted by a 0.4 M solution of nitric
175 acid. PIC was obtained considering a 1:1 stoichiometry between Ca^{2+} and PIC, i.e. all of the calcium on the
176 filters was considered to have come from calcium carbonate (Fagerbakke et al., 1994). POP was determined

177 as the difference between the total particulate phosphorus and particulate inorganic phosphorus, analyzed
178 using a auto-analyser Seal Analytical AA3, after the filters were placed in a solution of hydrochloric acid,
179 according to the method of Labry et al. (2013).

180

181 **2.2 Modelling**

182 **2.2.1 Monod and Droop model**

183 Growth of *E. huxleyi* in the batch reactors was simulated using Monod and Droop models of cellular
184 growth.

185 In the Monod model (Monod, 1949), the growth rate depends on the external nutrient concentration and is
186 calculated as:

$$187 \quad \mu = \mu_{\max} \cdot \frac{[R]}{[R] + K_R} \quad (1)$$

188

189 where μ_{\max} (in days⁻¹) is the maximum growth rate in nutrient-replete conditions, K_R (in $\mu\text{mol L}^{-1}$) is the
190 (Monod) half-saturation constant for growth and $[R]$ (in $\mu\text{mol L}^{-1}$) is the concentration of nutrient R in the
191 batch reactor. Both μ_{\max} and K_R were obtained by fitting the model to the data, while $[R]$ is the nutrient
192 concentration in the culture experiments calculated as detailed below.

193 Two differential equations keep track of the total cell abundance in the batch reactor (*Cells*) and the
194 limiting nutrient concentration in the reactor:

$$195 \quad \frac{d\text{Cells}}{dt} = \mu \cdot \text{Cells} \quad (2)$$

196

$$197 \quad \frac{d[R]}{dt} = \frac{-R_{UP} \cdot \text{Cells}}{V} \quad (3)$$

198 where V (in litres) is the volume of the batch reactor, *Cells* (in cells mL⁻¹) is the cell density measured during
199 the experiments, and R_{UP} the cell-specific R uptake rate (in $\mu\text{mol}_R \text{ cell}^{-1} \text{ d}^{-1}$) given by:

$$200 \quad R_{UP} = \mu \cdot Q_R \quad (4)$$

201

202 where Q_R , the (constant) cellular quota of nutrient R (in $\mu\text{mol}_R \text{ cell}^{-1}$) is the value of the quota R at the end
203 of the control experiment.

204

205 In the Droop model (Droop, 1968) nutrient uptake and cellular growth are decoupled and cellular growth
206 depends on the internal store of the limiting nutrient. The time-dependent rate of nutrient uptake, R_{up} (in
207 $\mu\text{mol}_R \text{ cell}^{-1} \text{ d}^{-1}$), is simulated using Michaelis-Menten uptake kinetics:

208
$$R_{up} = S_{cell} \cdot V_{maxR} \cdot \frac{[R]}{[R] + K_R} \quad (5)$$

209 where S_{cell} (in μm^3) is the surface area of the cell, V_{maxR} (in $\mu\text{mol}_R \mu\text{m}^{-2} \text{d}^{-1}$) is the maximum surface-
 210 normalized nutrient uptake rate (obtained by fitting the model to the data) and K_R (in $\mu\text{mol L}^{-1}$) is the
 211 (Michaelis-Menten) half-saturation constant for uptake of nutrient R. The volume and surface of cells (S_{cell})
 212 was obtained either by measurements of cells (both in the control culture and at the end of the nutrient-
 213 limited cultures) for the RCC911 strain experiments, or was estimated from Q_C , the cellular organic carbon
 214 quota (in $\text{pmol}_C \text{cell}^{-1}$), and the density of carbon in coccolithophore biomass (approximately equal to 0.015
 215 $\text{pmol}_C \mu\text{m}^{-3}$; Aloisi, 2015) for the batch experiments of Langer et al. (2013) for which cell measurements
 216 were not made.

217 The phytoplankton growth rate μ (in d^{-1}) was calculated based on the normalized ⁿQuota equation reported
 218 in Flynn (2008):

219
$$\mu = \mu_{max} \cdot \frac{(1 + KQ_R) \cdot (Q - Q_R^{min})}{(Q - Q_R^{min}) + KQ_R \cdot (Q_R^{max} - Q_R^{min})} \quad (6)$$

220
 221 where μ_{max} (in d^{-1}) is the maximum growth rate attained at the maximum nutrient cell quota Q_R^{max} (in μmol
 222 cell^{-1}), Q_R^{min} (in $\mu\text{mol cell}^{-1}$) is the minimum (subsistence) cellular quota of nutrient R below which growth
 223 stops and KQ_R is a dimensionless parameter that can be readily compared between nutrient types and
 224 typically has different values for NO_3 and PO_4 (Flynn, 2008). While Q_R^{max} was obtained from the analysis of
 225 the nutrient quota (N or P) at the end of the control experiments, Q_R^{min} was estimated by calculation
 226 described in the Sect. 2.2.2 below and KQ_R was obtained from fitting the model to the experimental data.
 227 Thus, in the Droop model, the growth rate depends on the internal cellular quota of nutrient R, rather than
 228 on the external nutrient concentration like in the Monod model of phytoplankton growth.
 229 Three differential equations keep track of the total cell abundance in the batch reactor ($Cells$), the nutrient
 230 concentration in the reactor ($[R]$, in $\mu\text{mol L}^{-1}$) and the internal cellular quota of nutrient (Q_R , in $\mu\text{mol cell}^{-1}$):

231
$$\frac{dCells}{dt} = \mu \cdot Cells \quad (7)$$

232
 233
$$\frac{d[R]}{dt} = \frac{-N_{up} \cdot Cells}{V} \quad (8)$$

234
 235
$$\frac{dQ_R}{dt} = N_{up} - \mu \cdot Q_R \quad (9)$$

236

237 These three differential equations are integrated forward in time starting from initial conditions chosen
238 based on experimental values of the number of cells, nutrient concentration at the beginning of the
239 experiment and the cellular nutrient quota determined during growth in nutrient-replete conditions.

240

241 The dependence of the maximum growth rate on irradiance was determined independently by fitting the
242 growth rate determined in the exponential growth phase in our experiments and in the experiment of
243 Langer et al. (2013) to the following equation from MacIntyre et al. (2002):

$$244 \quad \mu = \mu_{\max} \left(1 - e^{\left(\frac{-Irr}{K_{Irr}} \right)} \right) \quad (10)$$

245

246 where K_{Irr} is the light-saturation parameter of growth in $\mu\text{mol photons m}^{-2} \text{s}^{-1}$ (MacIntyre et al., 2002; Fig.
247 S1) and was determined by this equation.

248

249 **2.2.2 Modelling strategy**

250 The Droop model presented here does not take into account the variation of size of coccolithophore
251 cells between the different experiments. This model has eight parameters. Four are considered to be
252 known and constant for a given experiment: batch volume V , cell volume (and surface area S_{cell}), and
253 minimum and maximum cellular quota of nutrient, respectively Q_{min} and Q_{max} . The unknown parameters
254 (the physiological parameters of interest) are: the (Michaelis-Menten) half-saturation constant for nutrient
255 uptake K_R , the maximum surface-normalized nutrient uptake rate V_{maxR} , the maximum growth rate μ_{max} and
256 the dimensionless parameter KQ_R . The Monod model has fewer known parameters: batch volume V and
257 cellular quota of nutrient Q_R . Unknown parameters are: maximum growth rate μ_{max} and the (Monod) half-
258 saturation constant for growth K_R .

259 Concerning Q_R^{\min} , the measured minimum PON value ($5.71 \text{ fmol cell}^{-1}$) for the N-limited experiment of
260 Langer et al. (2013) is very low compared with the PON quota in other N-limited *E. huxleyi* experiments
261 reported in the literature ($38.9\text{-}39.3 \text{ fmol cell}^{-1}$ in Sciandra et al., 2003; and $51.4 \text{ fmol cell}^{-1}$ in Rouco et al.,
262 2013). When the Q_N^{\min} value of Langer et al. (2013) was used in the model, the model fit to the
263 experimental data degraded considerably (data not shown). Consequently, we decided to recalculate Q_N^{\min}
264 using the initial concentration of dissolved N and the final cell density in the reactor (column "Calculation"
265 in Table 3). This calculated value of Q_N^{\min} , that in all cases except for the N-limited experiments of Langer et
266 al. (2013) was very similar to the measured minimum PON quota, was comparable to values reported in the
267 literature for *E. huxleyi* and resulted in a very good fit of the model to the experimental data. To be
268 coherent, we applied this approach to all values of Q_N^{\min} and Q_p^{\min} used in the modelling exercise.

269 A point to note concerning the Q_p^{\max} used for the P-limited experiment of Langer et al. (2013) is that the
270 initial C:P ratio for the control experiment was 214, which is much higher than the Redfield ratio of 106

271 (Redfield, 1963). It is not possible to reproduce the experimental data when imposing such a high C:P ratio
272 in the model. Thus, the Q_p^{\max} value had to be increased in order to reproduce the data and thus estimate
273 additional physiological parameters for this experiment. For this reason, the modelling results for this
274 particular experiment should be taken with caution.

275

276 The time-dependent cell density, limiting nutrient concentration and cellular particulate organic
277 nitrogen and phosphorus calculated by the models were fitted to the same quantities measured in the
278 experiments. For our experiments there were only two nutrient cellular quota data points, one at the
279 beginning and one at the end of the experiments. We artificially inserted a third nutrient-quota data point
280 at the end of the exponential growth phase, setting it equal to the nutrient quota at the beginning of the
281 experiment. In this way the model is forced to keep the nutrient quota unchanged during the exponential
282 growth phase. This is a reasonable assumption, as cellular nutrient quotas should start to be affected only
283 when nutrient conditions become limiting.

284 The quality of the model fit to the experimental data was evaluated with a cost function. For a given model
285 run, the total cost function was calculated as follows:

$$286 \quad TotCost = \sum_{i=1}^n (\Delta x_i)^2 \quad (11)$$

287 where n is the number of data points available and ΔX_i is the difference between the data and the model
288 for the i^{th} data point:

$$289 \quad \Delta x_i = Data(x_i) - Model(x_i) \quad (12)$$

290 where X_i is the data or model value for the considered variable (cell density, limiting nutrient concentration
291 or cellular limiting nutrient quota). The lower the cost function is, the better the quality of the model fit to
292 the data. For a given experiment, the best-fit of the model to the data was obtained by running the model
293 repeatedly imposing a high number of combinations of input parameters (typically 500000 model runs for
294 every experiment) and selecting the parameter setting that yielded the lowest cost.

295

296 **3. Results**

297 **3.1 Laboratory experiments with *E. huxleyi* strain RCC911**

298 Growth curves for all experiments with *E. huxleyi* strain RCC911 are shown in Fig. 1. Experiments run in
299 high light conditions attained target cell densities (in nutrient-replete, control experiments) or nutrient
300 limitation (in nutrient-limited experiments) in a shorter time compared to experiments run in low light
301 conditions. Growth in nutrient-replete cultures in both light conditions followed an exponential growth

302 curve (growth rates in the control nutrient-replete experiments were $0.91 \pm 0.03 \text{ d}^{-1}$ and $0.28 \pm 0.01 \text{ d}^{-1}$ for
303 the high light and low light experiments, respectively; Table 1) whereas in nutrient-limited experiments
304 growth evolved from an exponential to a stationary phase at the end of the experiment, except the P-
305 limited culture at low light where the stationary phase was not attained (growth rate of $0.13 \pm 0.01 \text{ d}^{-1}$).
306

307 In the high light experiment, NO_3 concentration decreased to $0.18 \pm 0.03 \text{ }\mu\text{M}$ in N-limited cultures and
308 PO_4 concentration decreased to $0.011 \pm 0.004 \text{ }\mu\text{M}$ in P-limited cultures at the end of the experiments, and
309 in low light conditions the final NO_3 and PO_4 concentrations were $0.13 \pm 0.02 \text{ }\mu\text{M}$ and $0.008 \pm 0.006 \text{ }\mu\text{M}$,
310 respectively (Table 1). Thus, nutrients were nearly completely exhausted at the end of our nutrient-limited
311 experiments. Seawater carbonate chemistry was quasi-constant over the course of the experiments in all
312 treatments, with, as reported by Langer et al. (2013), the P-limited cultures undergoing the largest change
313 in DIC (12-13%; Table 1).

314 Compared to the control experiments, cellular POC, PIC and PON quotas increased in the P-limited
315 cultures at both light levels, while cellular POP quota decreased (Table 2; Fig. 2D). In the N-limited cultures,
316 cellular PIC and POC quotas (Fig. 2A and B) increased, with the exception of POC at low light that remained
317 nearly unchanged, while cellular PON and POP quotas (Fig. 2C and D) decreased at both light levels. N-
318 limiting conditions resulted in an increase of the POC:PON ratio in both light regimes (Fig. 3A, Table 2).
319 POC:POP (Fig. 3B) was higher in P-limited experiments compared to nutrient-replete experiments. The
320 PIC:POC ratio increased with both N- and P-limitation (Fig. 3C) at both light regimes. For the high light
321 experiment, the PIC:POC ratio was highest in the P-limited culture (0.52 ± 0.14), while in the low light
322 conditions, the highest ratio was recorded in the N-limited culture (0.33 ± 0.02) (Fig. 3C).

323 Light limitation led almost invariably to a decrease in POC and PIC, with the exception of POC in
324 nutrient-replete conditions (Table 2, Fig. 2). In P-limited cultures POP and PON decreased with light
325 limitation, whereas in N-limited cultures POP and PON increased with light limitation (Fig. 2). With the
326 exception of the POC:POP ratio in P-limiting conditions that was not affected by the change in light regime,
327 both POC:PON and POC:POP ratios decreased with light limitation. Finally, the PIC:POC ratio decreased with
328 light limitation in all three nutrient conditions.

329
330 Cell size varied with both nutrient and light limitation (Table S1). Compared to the control culture, in
331 high light conditions, the cell volume was higher for the P-limited culture ($77.2 \pm 19.9 \text{ }\mu\text{m}^3$) and was similar
332 for the N-limited culture ($47.33 \pm 11.13 \text{ }\mu\text{m}^3$). The same pattern was observed in low light conditions. P-
333 limitation resulted in higher coccosphere volume and higher DSL than the other nutrient conditions in both
334 light regimes (Table S1). For example, the coccosphere volume in high light was $260 \pm 88 \text{ }\mu\text{m}^3$ for the P-
335 limited experiment, whereas it was $109 \pm 23 \text{ }\mu\text{m}^3$ for the control experiment and $139 \pm 41 \text{ }\mu\text{m}^3$ for the N-
336 limited experiment. There was no measurement of coccosphere volume and DSL in the low light control
337 culture because of a lack of visible cells on the filters. However, the coccosphere volume for the P-limited

338 treatment followed the same trend as the cell size, i.e. a decrease with lower light. Figure 4A shows the
339 correlation between POC content and cell volume ($R^2=0.85$, $p<0.05$, $n=6$) and figure 4B between cell and
340 coccosphere volume ($R^2=0.92$, $p<0.03$, $n=5$). Relationships between DSL and coccosphere size ($R^2=0.68$,
341 $p<0.3$, $n=5$) and between DSL and cell size ($R^2=0.86$, $p<0.06$, $n=5$) are illustrated in figure 4C. These
342 parameters were not significantly correlated, but the sample size was rather low. The thickness of the
343 coccolith layer, calculated by subtracting the cell diameter from the coccosphere diameter and dividing by
344 two, was higher for P-limited cultures in both light conditions: $1.294 \pm 0.099 \mu\text{m}$ for high light and $1.02 \pm$
345 $0.043 \mu\text{m}$ for low light compared with the other cultures which were between 0.66 and $1 \mu\text{m}$. These
346 observations are consistent with the high PIC quota and relatively large size of coccospheres and coccoliths
347 of *E. huxleyi* under P-limitation.

348

349 **3.2 Modelling results**

350 We applied the modelling approach to both the data from our batch culture experiments with strain
351 RCC911 and to the batch culture data of Langer et al. (2013) who tested N- and P-limited growth of *E.*
352 *huxleyi* strain PML B92/11 cultured in high light conditions ($400 \mu\text{mol photons m}^{-2} \text{ s}^{-1}$), optimal temperature
353 (15°C) and quasi-constant carbon system conditions. Measurements of cell density, nutrient concentrations
354 and cellular particulate matter from both sets of experiments were used for the present modelling study.

355 The Droop model was able to accurately reproduce both experimental data sets (Fig. 5, 6 and 9; Fig.
356 S2, S3 and S4), whereas the Monod model was not able to reproduce the rise in cell number after the
357 limiting nutrient had been exhausted (Fig. 5). The modelling approach allows evaluation of the evolution of
358 experimental variables that are complicated to determine analytically, i.e. (1) the nutrient-uptake rate, that
359 follows the same trend as the nutrient concentration in the reactor, (2) the C/limited-nutrient ratio, that
360 starts at a minimum value, stays constant during the duration of the exponential phase and then increases
361 due to exhaustion of the external nutrient, reaching a maximum as the culture attains the stationary phase,
362 and (3) the instantaneous growth rate, that follows the trend of the limiting nutrient ratio, reaching zero
363 when the culture attains the stationary phase.

364

365 The values for the physiological parameters of the best-fit obtained by applying the Droop model to
366 our experiments with *E. huxleyi* strain RCC911 and to the experiments of Langer et al. (2013) are presented
367 in Table 3. Overall, the best-fit values for the two strains in high light conditions were very similar,
368 suggesting that the modelling approach is sound. Values for the half-saturation constant for nitrate uptake
369 K_N determined in our experiments in high light conditions and in those of Langer et al. (2013) were
370 comparable. However, for K_p , the value was consistent between our high and low light experiments, but
371 considerably lower for the Langer et al. (2013) experiment, which, as noted above, is a result that should be
372 taken with caution. The maximum surface nutrient-uptake rate V_{max} were similar between our high light
373 experiment and that of Langer et al. (2013). The dimensionless parameters KQ_N and KQ_p were also

374 comparable between the two studies for high light conditions and in both cases KQ_p was higher than KQ_N .
375 Maximum growth rates in high light conditions were similar for both N-limited and P-limited experiments.
376 As expected, maximum growth rates for our low light cultures were considerably lower (Table 3).

377 To test the reliability of the model to obtain estimates of the physiological parameters, we forced the
378 model to run with a range of values for a given parameter, while letting the other three parameters vary
379 over a wide range. These tests give us plots of the value of the cost function (Eq. 9) as a function of the
380 value of the imposed parameter. The process was repeated separately for the four unknown parameters
381 and Fig. S5 shows the results for the N-limited culture of Langer et al. (2013). For all of the parameters
382 except for K_R , this exercise yielded a U-shaped curve with a minimum of the cost function corresponding to
383 the best-fit parameter values presented in Table 3. This shows that the model is well suited to find a best-fit
384 value for these parameters. Three minima of the cost function were found for K_R (Fig. S5) of which only the
385 lowest was consistent with values reported in the literature (e.g. Riegman et al., 2000). This value was
386 chosen to obtain the best-fit of the model to the experimental data.

387

388 4. Discussion

389 4.1 Batch culture experiments

390 The batch culture experiments presented here provide new insights into the physiology of the
391 numerically dominant coccolithophore *E. huxleyi* under conditions of light and nutrient limitation.
392 Leonardos and Geider (2005) carried out cultures in low light and low phosphate conditions with a non-
393 calcifying *E. huxleyi* strain and thus did not report PIC:POC ratios. The culture study reported here is thus
394 the first experiment where changes in the PIC:POC ratio due to light-limitation are explored for nutrient-
395 limited cultures. In our experiments, cultures were harvested at relatively low cell densities, i.e. a maximum
396 of ca. $1.6 \cdot 10^5$ cells mL^{-1} in the P-limited low light experiment and $< 1.3 \cdot 10^5$ cells mL^{-1} in all other
397 treatments. The aim was to ensure that changes in the carbonate system were within a minimal range ($<$
398 10% except for the P-limited experiments in which the DIC changes were 12 and 13%; Table 1) that is not
399 expected to have a significant influence on measured physiological parameters (Langer et al., 2007;
400 LaRoche et al., 2010). Hence, it can be stated that the observed phenomena stem from N-/P-limitation
401 and/or light limitation (depending on the treatment) rather than from carbon limitation.

402 Comparison of the growth curves illustrated in Fig. 1 demonstrates that growth limitation was attained
403 in both our low nutrient and low light treatments relative to control conditions. Consistent with previous
404 experimental results (Langer et al., 2013; Leonardos and Geider, 2005; Müller et al., 2012; Oviedo et al.,
405 2014; Rouco et al., 2013), the relatively low cellular PON or POP quotas (and high POC:PON and POC:POP
406 ratios) at the end of the low nutrient experiments relative to the control indicate that nutrient limitation of
407 growth occurred in our low nutrient experiments. The stationary phase was not attained in the P-limited
408 low light culture, but it can be inferred that cells were P-limited from: (a) the POP quota, which was lower

409 than that of the control, (b) the POC:POP ratio, which was higher than that of the control, and (c) a
410 deviation of the growth curve from exponential growth starting (at the latest) on day 16 of 19. While a
411 decline in POP quota is an early sign of limitation, the decline in growth rate occurs later, indicating more
412 severe limitation. The cessation of cell division (stationary phase) would be the last stage in the process of
413 becoming fully P-limited over the course of a batch culture.

414

415 In nutrient-replete conditions, low light had no effect on POC quota (Fig. 2) and cell size (Fig. 4) within
416 the limit of uncertainty of the measurements, whereas it caused a decrease in PIC quota (and therefore a
417 decrease in PIC:POC ratio). Although PIC quota also decreased in low light for nutrient-limited conditions
418 (Fig. 2), the PIC quota for nutrient-replete conditions in low light was unexpectedly low indicating a
419 potential anomaly in the calcification process for this experiment.

420 In our experiments N-limitation led to an increase in the PIC:POC ratio in both high and low light
421 conditions, a result that is consistent with most previous N-limitation studies with *E. huxleyi* (see review by
422 Raven and Crawford, 2012), but the cause of this increase appears to vary. According to Müller et al. (2008)
423 and Raven and Crawford (2012), N-limited cells decrease in volume due to substrate limitation and lower
424 assimilation of nitrogen in the G1 phase of the cell division cycle, but in our experiments N-limitation did
425 not cause an obvious decrease in cell volume or POC quota, but rather an increase in PIC quota relative to
426 nutrient-replete cells in both high and low light conditions (Fig. 2) (Table S1). Both Müller et al. (2008) and
427 Fritz (1999) also reported an increase of the PIC content of *E. huxleyi* in N-limited conditions. The increase
428 in PIC quota is difficult to explain in light of the observations that coccolith size was lower in N-limited
429 cultures and coccosphere volume was broadly comparable (given the error margins) in control and N-
430 limited cultures (Fig. 4).

431 P-limitation had the greatest effect on cell size, cells being significantly larger under P-limitation than
432 in control conditions, for both high and low light regimes. The increase in cell volume was accompanied by
433 increases in both POC and PIC quotas, again in both light conditions (Fig. 2). According to Müller et al.
434 (2008), P-limitation inhibits DNA replication while biomass continues to build up, leading to an increase in
435 cell volume. This could explain the very high volume of P-limited cells in high light conditions in our
436 experiments, and the slightly increased cell volume in the P-limited, low light experiment, compared to
437 experiments not limited by PO_4 . P-limitation resulted in a considerably higher coccosphere volume than the
438 other nutrient conditions, in line with the observations of Müller et al. (2008) and Oviedo et al. (2014). In
439 high light the PIC quota in P-limited cells was more than tripled relative to nutrient-replete conditions. This
440 general effect of phosphate limitation was also reported by Raven and Crawford (2012) (Table 2) and is
441 likely due to the occurrence of larger (as shown by high DSL values) and potentially more numerous
442 coccoliths (Gibbs et al., 2013). In the P-limited experiment, PIC:POC ratios increased relative to nutrient-
443 replete cultures, like in the experiments of van Bleijswijk et al. (1994) and Berry et al. (2002), although
444 Oviedo et al. (2014) reported that the response of the PIC:POC ratio to P-limitation is strain-specific in *E.*

445 *huxleyi*. The increase in PIC:POC in *E. huxleyi* is often greater for P-limitation than for N-limitation
446 (Zondervan, 2007), as for our high light experiment. However, in low light the PIC:POC ratio was higher
447 under N-limitation, highlighting that co-limitation can have unexpected physiological consequences.

448

449 In our experiments the PIC:POC ratio decreased with light limitation in nutrient replete and nutrient
450 limited conditions (Fig. 3). Zondervan (2007) stated that the ratio of calcification to photosynthetic C
451 fixation increases with decreasing light intensities due to the lower saturation irradiance for calcification
452 than photosynthesis in *E. huxleyi*. However, due to a more rapid decline of calcification relative to
453 photosynthesis below saturation levels this ratio decreases again under strongly light-limiting conditions
454 (below approximately $30 \mu\text{mol photons m}^{-2} \text{s}^{-1}$). Several culture studies using different *E. huxleyi* strains
455 have reported this trend. Using the same L:D cycle (12:12) as employed in our experiments, Feng et al.
456 (2008) also reported a decreasing PIC:POC ratio between 400 and $50 \mu\text{mol photons m}^{-2} \text{s}^{-1}$. Comparable
457 observations have been reported in studies that used a 16:8 L:D cycle with decreasing light from 300 down
458 to a minimum of $30 \mu\text{mol photons m}^{-2} \text{s}^{-1}$ (Trimborn et al., 2007; Rokitta and Rost, 2012). Again with a 16:8
459 L:D cycle, Rost et al. (2002) reported a decrease of the PIC:POC ratio between 80 and $15 \mu\text{mol photons m}^{-2}$
460 s^{-1} (for a pCO_2 level comparable to that in our experiments), but with an increase of the ratio from 150 to 80
461 $\mu\text{mol.m}^{-2}.\text{s}^{-1}$. Our results indicate that calcification was more severely limited than photosynthesis at 30
462 $\mu\text{mol photons m}^{-2} \text{s}^{-1}$ in strain RCC911.

463 The non-significant correlation between DSL and coccosphere size (Fig. 4) is not consistent with the
464 correlation reported by Gibbs et al. (2013) between coccolith and coccosphere size in fossil sediment
465 samples, but the number of observations in our study was too low to draw a robust conclusion about the
466 relationship. The significant correlation between cell and coccosphere volume (Fig. 4) and observations of
467 other studies (e.g. Aloisi, 2015; Gibbs et al., 2013) support the conclusion that coccosphere size in the water
468 column and in sediments could be used as a proxy for cell size (and thus POC quota).

469

470 In summary, apart from the phosphate limited low light experiment, nutrient limitation led to a
471 cessation of cell division (entry into stationary phase) at the end of the experiment. Nutrient limitation
472 decreased the particulate organic P or N quota for the limiting nutrient (POP for P-limitation and PON for N-
473 limitation) and increased the PIC:POC ratio under both light conditions. Discerning the effect of nutrient
474 limitation on morphological properties was complicated by the relatively large margins of error, but the
475 overall trend was of an increase in cell/coccosphere size under P-limitation and no obvious effect under N-
476 limitation. Light limitation decreased the PIC quota, tended to decrease the cell size and decreased PIC:POC
477 ratio in every nutrient condition, whereas POC:PON and POC:POP decreased with light limitation. Further
478 investigations need to be carried out to improve the understanding of the effect of light intensity on the
479 PIC:POC ratio.

480

481 **4.2 *E. huxleyi* physiological parameters obtained by modelling growth in a batch reactor**

482 In contrast to the Monod model, the Droop model was able to accurately reproduce the experimental
483 data obtained in experiments with *E. huxleyi* strain RCC911 as well as the experiments of Langer et al.
484 (2013). The Droop model was notably able to reproduce the increase in cell number after the limiting
485 nutrient had been exhausted. This indicates that, as for several other phytoplankton groups (Lomas and
486 Glibert, 2000), *E. huxleyi* has the ability to store nutrients internally to continue growth to some extent
487 when external nutrient levels become very low. In our experiments and those of Langer et al. (2013), cells
488 grew on their internal nutrient reserves and managed two to three cell divisions in the absence of external
489 nutrients. These observations are consistent with the explanation of both Monod and Droop models by
490 Bernard (2011).

491 Numerous studies have estimated the maximum nutrient uptake rate $V_{\max R}$ and the half-saturation
492 constant for nutrient uptake K_R , especially for nitrate uptake, for a variety of phytoplankton species. The
493 values obtained in our study for K_N for high light *E. huxleyi* cultures (Table 3) are comparable to those
494 reported in the literature. Using *E. huxleyi* in chemostat experiments, Riegman et al. (2000) found K_N values
495 between 0.18 and 0.24 μM and K_p between 0.10 and 0.47 μM . In addition, they reported a $V_{\max N}$ of $7.4 \cdot 10^{-6}$
496 $\mu\text{mol cell}^{-1} \text{d}^{-1}$ which is similar to that found for RCC911 and PML B92/11 (Table 3).

497 When comparing physiological parameters between phytoplankton taxa, the scaling of physiological
498 parameters with cell size has to be taken into account (Marañón et al., 2013). Marañón et al. (2013) plotted
499 Q_{\min} and μ_{\max} against cell size (see Fig. 7A for Q_{\min} versus cell size) for different phytoplankton species. In
500 these plots coccolithophores fall with the smallest diatoms. Figure 7B reports $V_{\max N}$ versus cell size for
501 different groups of phytoplankton based on the results of Litchman et al. (2007) (using a compiled
502 database) and of Marañón et al. (2013) (22 cultivated species) and the results obtained with the Droop
503 model in this study. Despite the different procedures used to obtain $V_{\max N}$ (simulated with a model or
504 measured experimentally), all values for coccolithophores fall in the same range. Collos et al. (2005) and
505 Litchman et al. (2007) found a linear correlation between the maximum uptake rate and the half-saturation
506 constant for nitrate uptake across several phytoplankton groups (Fig. 7C). This correlation defines a
507 physiological trade-off between the capacity to assimilate nutrients efficiently (high V_{\max}) and the capacity
508 to assimilate nutrients in low-nutrient environments (low K_R), and thus thrive in oligotrophic conditions.
509 This analysis shows that large phytoplankton like diatoms and dinoflagellates have high maximum nitrate
510 uptake rates and high half-saturation constant for nitrate uptake. The half-saturation constant for nitrate
511 uptake for *E. huxleyi* is consistently low compared to other groups of phytoplankton, which means that it
512 will be competitive in low nitrate waters (Litchman et al., 2007).

513

514 **4.3 Controls on *E. huxleyi* growth in the deep BIOSOPE niche**

515 The BIOSOPE cruise was carried out in 2004 along a transect across the South Pacific Gyre from the
516 Marquesas Islands to the Peru-Chili upwelling zone. The aim of this expedition was to study the biological,

517 biogeochemical and bio-optical properties (Claustre et al., 2008) of the most oligotrophic zone of the
518 world's ocean (Claustre and Maritorena, 2003). The deep ecological niche of coccolithophores along this
519 transect occurred at the Deep Chlorophyll Maximum (DCM; Beaufort et al., 2008). According to Claustre et
520 al. (2008) and Raimbault et al. (2008), the nitrate concentration at the GYR station at the DCM (between
521 150 and 200 m depth) was between 0.01 and 1 μM . In our nitrate-limited low light culture experiment (Fig.
522 8), this concentration occurred between the end of the exponential growth phase and the beginning of the
523 stationary phase (days 8 to 9), when nitrate-limitation began to affect instantaneous growth rates. Claustre
524 et al. (2008) reported a nitrate concentration <3 nM (i.e. below the detection limit) in the 0-100 m water
525 column, whereas phosphate concentration was always above 0.1 μM in surface layers (Raimbault and
526 Garcia, 2008). Moutin et al. (2008) concluded that phosphate was apparently not the limiting nutrient for
527 phytoplankton along the BIOSOPE transect. A potential influence of organic nitrogen sources, that *E.*
528 *huxleyi* is capable of using (Benner and Passow, 2010), cannot be excluded, but these would be expected to
529 have been distributed vertically in a similar way to NO_3 .

530 The picture that emerges from the figure 9 is consistent with the model of Klausmeier and Litchman
531 (2001), who predicted that growth in a DCM should be limited by both light and one nutrient, with the
532 upper layer of the DCM being limited by nutrient supply and the deeper layer by light. The experiments and
533 modelling work presented here allow us to confirm that growth of *E. huxleyi* in the deep niche at the GYR
534 station of the BIOSOPE transect was clearly limited by light in the lower part of the DCM, and by nitrogen in
535 the upper part of the DCM and upper water column. Nitrification and the vertical diffusivity of nitrate
536 through the nitracline (Holligan et al., 1984) needs to be taken into account and could potentially be a
537 source of dissolved nitrate in the deep niche of coccolithophores. The depth-distribution of the modelled *E.*
538 *huxleyi* growth rate, and of dissolved nitrogen, light intensity, chlorophyll a concentration and
539 coccolithophore abundance supports the inferred light-nitrate co-limitation (Fig. 9). We used the
540 physiological parameters constrained in our experiments together with a steady state assumption for
541 uptake and assimilation of nitrate (see appendix) to obtain the vertical profile of *E. huxleyi* growth rate at
542 the GYR station (Fig. 9). This calculation, forced by the irradiance and nitrate data from the GYR station,
543 shows that *E. huxleyi* growth rate was maximal at a depth corresponding to that of the measured maximum
544 chlorophyll a concentration. The half-saturation constant for nitrate uptake K_N constrained with the Droop
545 model (0.09 μM) lies within the deep niche (Fig. 9). The maximum estimated growth rate at the GYR station
546 (0.024 d^{-1} at 175 m depth) corresponds to an *E. huxleyi* generation time of 29.3 days, suggesting that
547 division rate at the DCM was extremely slow, all the more so since this estimate does not consider grazing
548 and vertical export of cells. Reports of the in situ growth rate of phytoplankton are not common, including
549 for *E. huxleyi*, due to the inherent difficulties in measuring this parameter (Laws, 2013). Goldman et al.
550 (1979) reported phytoplankton doubling times in the North Pacific around 0.36-0.89 per day which
551 corresponds to a growth rate of approximately 0.25 d^{-1} . Selph et al. (2011) estimated growth rates in the

552 equatorial Pacific between 110° and 140°W to be below 0.3 d⁻¹ for the phytoplankton community living at
553 1% of surface irradiance with net growth rates (considering mortality rates) around zero.

554

555 With the above limitation pattern in mind, it is possible to predict the effect of nitrate and light
556 variability on the vertical evolution of the *E. huxleyi* PIC:POC ratio in gyre conditions. According to our
557 experimental results, the PIC:POC ratio increases slightly with nitrate limitation but the strongest effect on
558 PIC:POC ratio seems to be in response to light intensity. As noted above (Section 4.1), several studies have
559 shown that the PIC:POC ratio increases with decreasing irradiance down to $55 \pm 25 \mu\text{mol photons m}^{-2} \text{ s}^{-1}$,
560 but that it decreases with light limitation below this value. At the BIOSOPE GYR station, the PIC:POC ratio of
561 *E. huxleyi* would be expected to be intermediate in surface waters (nitrate-poor but high light intensity) and
562 then to increase and attain a maximum value in lower subsurface waters down to the upper part of the
563 deep niche (between 80 and 30 $\mu\text{mol photons m}^{-2} \text{ s}^{-1}$; therefore between 110 m and 150 m depth). The
564 PIC:POC ratio would then decrease in the lower part of the deep niche, and finally decrease drastically in
565 deeper, relatively nitrate-rich but extremely low-irradiance waters. This prediction cannot be verified with
566 the available published data from the BIOSOPE transect, but a comparable pattern for the upper part of the
567 ocean was observed through in situ measurements by Fernández et al. (1993). Our predictions need to be
568 verified via in situ studies of DCM zones dominated by coccolithophores. Klaas and Archer (2002) reported
569 that coccolithophores are responsible for the main part of calcium carbonate export to the deep sea and
570 that the rain of organic carbon is mostly associated with calcium carbonate particles, because of their
571 higher density than opal particles and higher abundance than terrigenous material. The gyre ecosystem is a
572 good example of the fact that effects on the rain ratio, and therefore on the carbon pump and carbonate
573 counter-pump, need to be integrated over the whole photic zone. A low PIC quota due to the majority of
574 production occurring at low irradiance in the deep niche would limit the *E. huxleyi*-related calcium
575 carbonate rain to the sediments and potentially also the ballasting of organic carbon to the deep ocean.

576

577 **5. Conclusion**

578 We present one of the few laboratory culture experiments investigating the growth and PIC:POC ratio
579 of the coccolithophore *E. huxleyi* in light- and nutrient-limited conditions, mimicking those of the deep
580 ecological niche of coccolithophores in the South Pacific Gyre (Beaufort et al., 2008; Claustre et al., 2008).
581 By combining batch culture experiments with a simple numerical model based on the internal stores
582 (Droop) concept, we show that: (1) *E. huxleyi* has the capacity to divide up to several times in the absence
583 of external nutrients by using internal nutrient stores; (2) a simple batch culture experimental set-up
584 combined with a Droop model, as opposed to the more time-consuming and expensive continuous culture
585 approach, can be used to estimate fundamental physiological parameters that describe the response of
586 phytoplankton growth to nutrient availability; (3) the position of the deep coccolithophore niche of the
587 South Pacific Gyre coincides with the depth of maximum potential growth rate calculated by our

588 physiological model; at shallower depths growth is strongly limited by dissolved nitrate availability, while at
589 greater depths it is strongly limited by the paucity of light. These observations confirm the theoretical
590 prediction of Klausmeier and Litchman (2001) with regard to the environmental controls of growth in the
591 DCM. Our conclusions were based on experiments using *E. huxleyi* strain RCC911 that was isolated from
592 surface waters of the BIOSOPE transect and it will be important to repeat this approach using deep-
593 dwelling strains. There is potential for our approach to shed light on the functioning of other oligotrophic,
594 low-light phytoplankton ecosystems like cold, dark and nutrient-poor Arctic and Antarctic waters.

595 Appendix

596

597 To obtain the growth rate through the vertical profile at the station GYR, we needed to express the
598 cellular quota Q_N as a function of the nitrate concentration $\text{NO}_3 [N]$. To achieve this, we resolved the system
599 of three equations from the Droop theory:

600

$$601 \quad \frac{dQ_N}{dt} = N_{up} - \mu \cdot Q_N \quad (\text{A1})$$

602

$$603 \quad N_{up} = S_{cell} \cdot V_{\max N} \cdot \frac{[N]}{[N] + K_N} \quad (\text{A2})$$

604

$$605 \quad \mu = \mu_{\max} \cdot \frac{(1 + KQ_N) \cdot (Q - Q_N^{\min})}{(Q - Q_N^{\min}) + KQ_N \cdot (Q_N^{\max} - Q_N^{\min})} \quad (\text{A3})$$

606

607 Considering a stationary state (uptake-assimilation steady state) and thus assuming the differential Eq. (A1)
608 equal to zero, we resolved the system to express the cellular quota Q_N versus the nitrate concentration (see
609 Fig. A1):

$$610 \quad A = \frac{1}{2 \cdot (1 + KQ_N) \cdot \mu_{\max} \cdot (K_N + [N])} \cdot \left((K_N \cdot (1 + KQ_N) \cdot \mu_{\max} \cdot Q_N^{\min}) \right) \quad (\text{A4})$$

611

$$612 \quad B = \left((1 + KQ_N) \cdot \mu_{\max} \cdot [N] \cdot Q_N^{\min} \right) + \left([N] \cdot S_{cell} \cdot V_{\max N} \right) \quad (\text{A5})$$

613

$$614 \quad C = \sqrt{4(1 + KQ_N) \cdot \mu_{\max} \cdot [N] \cdot (K_N + [N]) \cdot (KQ_N \cdot Q_N^{\max} - (1 + KQ_N) \cdot Q_N^{\min}) \cdot S_{cell} \cdot V_{\max N} + \left((1 + KQ_N) \cdot \mu_{\max} \cdot (K_N + [N]) \cdot Q_N^{\min} + [N] \cdot S_{cell} \cdot V_{\max N} \right)^2} \quad (\text{A6})$$

615

$$616 \quad Q_N = A \cdot (B + C) \quad (\text{A7})$$

617

618 Thus, the growth rate can be expressed depending on the irradiance (and $Klrr$; see Sect. 2.2.1) and the
 619 cellular quota Q_N . The other parameters are known (output of the model for the experiment reproducing
 620 the condition of the nitracline):

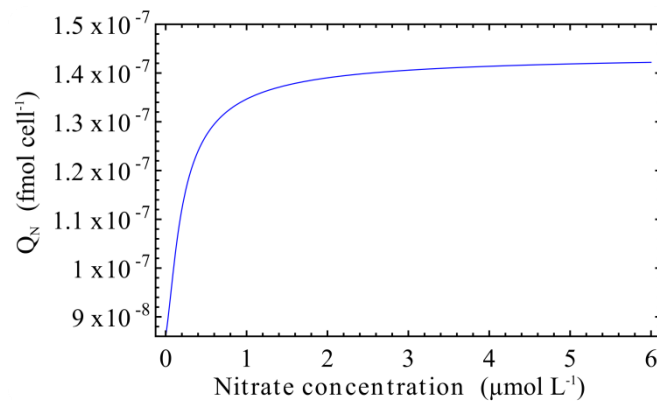
621

$$622 \quad \mu = \mu_{\max} \cdot \frac{(1 + KQ_N) \cdot (Q - Q_N^{\min})}{(Q - Q_N^{\min}) + KQ_N \cdot (Q_N^{\max} - Q_N^{\min})} \cdot \left(1 - e^{\left(\frac{-Irr}{Klrr} \right)} \right) \quad (A8)$$

623

624 The vertical profile of the growth rate of coccolithophores at the GYR station, calculated with this equation,
 625 is shown in Fig. 9.

626



627

628 *Figure A1.* Cellular quota of nitrogen versus the nitrate concentration using parameters of the best-fit results of the model ran for the low light and nitrate limited experiment with RCC911.

628

629 Acknowledgements

630

631 This project was supported by the TELLUS CLIMAHUX project (INSU-CNRS), the MODIF project of the
 632 Institut Pierre Simon Laplace (IPSL), and the CALHIS project (French ANR). We thank C. Schmechtig for
 633 providing access to the BIOSOPE database, F. Le Cornec and I. Djouaev for helping with PIC analysis at the
 634 Institut de Recherche pour le Développement (IRD) ALYSE platform and C. Labry and A. Youenou for
 635 carrying out the POP analysis at IFREMER Centre de Brest. From the Roscoff Biological Station we are
 636 grateful to C. Leroux for analysis of POC and PON samples and the Marine Chemistry research team,
 637 specifically T. Cariou for dissolved nutrient analyses and acid treatment of POC and PON samples, M. Vernet
 638 for help processing DIC samples, and Y. Bozec for DIC analysis. We also thank A. Charantonis for his advice
 639 for the modelling methodology. The lead author was supported by a doctoral fellowship from the French
 640 Minister of Education and Research (MESR).

641

642 **References**

- 643 Aloisi, G.: Covariation of metabolic rates and cell size in coccolithophores, *Biogeosciences*, 12(15), 6215–
644 6284, doi:10.5194/bg-12-4665-2015, 2015.
- 645 Beaufort, L., Couapel, M., Buchet, N., Claustre, H. and Goyet, C.: Calcite production by coccolithophores in
646 the south east Pacific Ocean, *Biogeosciences*, 5, 1101–1117, 2008.
- 647 Benner, I. and Passow, U.: Utilization of organic nutrients by coccolithophores, *Mar. Ecol. Prog. Ser.* 404,
648 21–29, 2010.
- 649 Bernard, O.: Hurdles and challenges for modelling and control of microalgae for CO₂ mitigation and biofuel
650 production, *J. Process Control*, 21(10), 1378–1389, doi:10.1016/j.jprocont.2011.07.012, 2011.
- 651 Berry, L., Taylor, A. R., Lucken, U., Ryan, K. P. and Brownlee, C.: Calcification and inorganic carbon
652 acquisition in coccolithophores, *Funct. Plant Biol.*, 29(3), 289–299, doi:10.1071/PP01218, 2002.
- 653 van Bleijswijk, J. D. L., Kempers, R. S., Veldhuis, M. J. and Westbroek, P.: Cell and growth characteristics of
654 types A and B of *Emiliana huxleyi* (Prymnesiophyceae) as determined by flow cytometry and chemical
655 Analyses, *J. Phycol.*, 30(2), 230–241, doi:10.1111/j.0022-3646.1994.00230.x, 1994.
- 656 Boyd, P. W., Strzepek, R., Fu, F. and Hutchins, D. A.: Environmental control of open-ocean phytoplankton
657 groups: Now and in the future, *Limnol. Oceanogr.*, 55(3), 1353–1376, doi:10.4319/lo.2010.55.3.1353, 2010.
- 658 Buitenhuis, E. T., Pangere, T., Franklin, D. J., Le Quéré, C. and Malin, G.: Growth rates of six coccolithophorid
659 strains as a function of temperature, *Limnol. Oceanogr.*, 53(3), 1181–1185, doi:10.4319/lo.2008.53.3.1181,
660 2008.
- 661 Claustre, H. and Maritorena, S.: The Many Shades of Ocean Blue, , 302(5650), 1514–1515, 2003.
- 662 Claustre, H., Sciandra, A. and Vaulot, D.: Introduction to the special section bio-optical and biogeochemical
663 conditions in the South East Pacific in late 2004: the BIOSOPE program, *Biogeosciences*, 5(3), 679–691,
664 doi:10.5194/bg-5-679-2008, 2008.
- 665 Cortés, M. Y., Bollmann, J. and Thierstein, H. R.: Coccolithophore ecology at the HOT station ALOHA, Hawaii,
666 *Deep Sea Res. Part II Top. Stud. Oceanogr.*, 48(8–9), 1957–1981, doi:10.1016/S0967-0645(00)00165-X,
667 2001.
- 668 Daniels, C. J., Sheward, R. M. and Poulton, A. J.: Biogeochemical implications of comparative growth rates
669 of *Emiliana huxleyi* and *Coccolithus* species, *Biogeosciences*, 11(23), 6915–6925, doi:10.5194/bg-11-6915-
670 2014, 2014.
- 671 Droop, M. R.: Vitamin B₁₂ and Marine Ecology. IV. The Kinetics of Uptake, Growth and Inhibition in
672 *Monochrysis Lutheri*, *J. Mar. Biol. Assoc. U. K.*, 48(3), 689–733, doi:10.1017/S0025315400019238, 1968.
- 673 Engel, A., Cisternas Novoa, C., Wurst, M., Endres, S., Tang, T., Schartau, M. and Lee, C.: No detectable effect
674 of CO₂ on elemental stoichiometry of *Emiliana huxleyi* in nutrient-limited, acclimated continuous cultures,
675 *Mar. Ecol. Prog. Ser.*, 507, 15–30, doi:10.3354/meps10824, 2014.
- 676 Eppley, R. W. and Renger, E. H.: Nitrogen Assimilation of an Oceanic Diatom in Nitrogen-Limited Continuous
677 Culture, *J. Phycol.*, 10(1), 15–23, doi:10.1111/j.1529-8817.1974.tb02671.x, 1974.
- 678 Eppley, R. W., Rogers, J. N. and McCarthy, J. J.: Half-Saturation Constants for Uptake of Nitrate and
679 Ammonium by Marine Phytoplankton, *Limnol. Oceanogr.*, 14(6), 912–920, doi:10.4319/lo.1969.14.6.0912,
680 1969.

681 Fagerbakke, K. M., Heldal, M., Norland, S., Heimdal, B. R. and Båtvik, H.: *Emiliana huxleyi*. Chemical
682 composition and size of coccoliths from enclosure experiments and a Norwegian fjord, *Sarsia*, 79(4), 349–
683 355, doi:10.1080/00364827.1994.10413566, 1994.

684 Feng, Y., Warner, M. E., Zhang, Y., Sun, J., Fu, F.-X., Rose, J. M. and Hutchins, D. A.: Interactive effects of
685 increased pCO₂, temperature and irradiance on the marine coccolithophore *Emiliana huxleyi*
686 (*Prymnesiophyceae*), *Eur. J. Phycol.*, 43(1), 87–98, doi:10.1080/09670260701664674, 2008.

687 Fernández, E., Boyd, P., Holligan, P. M. and Harbour: Production of organic and inorganic carbon within a
688 large-scale coccolithophore bloom in the northeast Atlantic Ocean, *Mar. Ecol. Prog. Ser.*, 97, 271–285,
689 1993.

690 Flynn, K.: The importance of the form of the quota curve and control of non-limiting nutrient transport in
691 phytoplankton models, *J. Plankton Res.*, 30(4), 423–438, doi:10.1093/plankt/fbn007, 2008.

692 Follows, M. J. and Dutkiewicz, S.: Modeling Diverse Communities of Marine Microbes, *Annu. Rev. Mar. Sci.*,
693 3(1), 427–451, doi:10.1146/annurev-marine-120709-142848, 2011.

694 Fritz, J. J.: Carbon fixation and coccolith detachment in the coccolithophore *Emiliana huxleyi* in nitrate-
695 limited cyclostats, *Mar. Biol.*, 133(3), 509–518, doi:10.1007/s002270050491, 1999.

696 Gibbs, S. J., Poulton, A. J., Brown, P. R., Daniels, C. J., Hopkins, J., Young, J. R., Jones, H. L., Thiemann, G. J.,
697 O’Dea, S. A. and Newsam, C.: Species-specific growth response of coccolithophores to Palaeocene–Eocene
698 environmental change, *Nat. Geosci.*, 6, 218–222, doi:10.1038/NGEO1719, 2013.

699 Goldman, J. C., McCarthy, J. J. and Peavey, D. G.: Growth rate influence on the chemical composition of
700 phytoplankton in oceanic waters, *Nature*, 279(2), 1, 1979.

701 Gregg, W. W. and Casey, N. W.: Modeling coccolithophores in the global oceans, *Deep Sea Res. Part II Top.*
702 *Stud. Oceanogr.*, 54(5–7), 447–477, doi:10.1016/j.dsr2.2006.12.007, 2007.

703 Haidar, A. T. and Thierstein, H. R.: Coccolithophore dynamics off Bermuda (N. Atlantic), *Deep Sea Res. Part*
704 *II Top. Stud. Oceanogr.*, 48(8–9), 1925–1956, doi:10.1016/S0967-0645(00)00169-7, 2001.

705 Henderiks, J., Winter, A., Elbrichter, M., Feistel, R., Plas, A. van der, Nausch, G. and Barlow, R.:
706 Environmental controls on *Emiliana huxleyi* morphotypes in the Benguela coastal upwelling system (SE
707 Atlantic), *Mar. Ecol. Prog. Ser.*, 448, 51–66, doi:10.3354/meps09535, 2012.

708 Holligan, P. M., Balch, W. M. and Yentsch, C. M.: The significance of subsurface chlorophyll, nitrite and
709 ammonium maxima in relation to nitrogen for phytoplankton growth in stratified waters of the Gulf of
710 Maine, *J. Mar. Res.*, 42(4), 1051–1073, doi:10.1357/002224084788520747, 1984.

711 Holligan, P. M., Fernández, E., Aiken, J., Balch, W. M., Boyd, P., Burkill, P. H., Finch, M., Groom, S. B., Malin,
712 G., Muller, K., Purdie, D. A., Robinson, C., Trees, C. C., Turner, S. M. and van der Wal, P.: A biogeochemical
713 study of the coccolithophore, *Emiliana huxleyi*, in the North Atlantic, *Glob. Biogeochem. Cycles*, 7(4), 879–
714 900, doi:10.1029/93GB01731, 1993.

715 Iglesias-Rodriguez, M. D., Halloran, P. R., Rickaby, R. E. M., Hall, I. R., Colmenero-Hidalgo, E., Gittins, J. R.,
716 Green, D. R. H., Tyrrell, T., Gibbs, S. J., von Dassow, P., Rehm, E., Armbrust, E. V. and Boessenkool, K. P.:
717 Phytoplankton calcification in a high-CO₂ world, *Science*, 320(5874), 336–340,
718 doi:10.1126/science.1154122, 2008.

719 Jordan, R. W. and Winter, A.: Assemblages of coccolithophorids and other living microplankton off the coast
720 of Puerto Rico during January–May 1995, *Mar. Micropaleontol.*, 39(1–4), 113–130, doi:10.1016/S0377-
721 8398(00)00017-7, 2000.

- 722 Kaffes, A.: Carbon and nitrogen fluxes in the marine coccolithophore *Emiliana huxleyi* grown under
723 different nitrate concentrations, *J. Exp. Mar. Biol. Ecol.*, 393, 1–8, doi:10.1016/j.jembe.2010.06.004, 2010.
- 724 Keller, M., Selvin, R., Claus, W. and Guillard, R.: Media for the culture of oceanic ultraphytoplankton, *J.*
725 *Phycol.*, 23, 633–638, 1987.
- 726 Klaas, C. and Archer, D. E.: Association of sinking organic matter with various types of mineral ballast in the
727 deep sea: Implications for the rain ratio, *Glob. Biogeochem. Cycles*, 16(4), 1116,
728 doi:10.1029/2001GB001765, 2002.
- 729 Klausmeier, C. A. and Litchman, E.: Algal games: The vertical distribution of phytoplankton in poorly mixed
730 water columns, *Limnol Ocean.*, 46(8), 1998–2007, 2001.
- 731 Krug, S. A., Schulz, K. G. and Riebesell, U.: Effects of changes in carbonate chemistry speciation on
732 *Coccolithus braarudii*: a discussion of coccolithophorid sensitivities, *Biogeosciences*, 8(3), 771–777,
733 doi:10.5194/bg-8-771-2011, 2011.
- 734 Labry, C., Youenou, A., Delmas, D. and Michelon, P.: Addressing the measurement of particulate organic
735 and inorganic phosphorus in estuarine and coastal waters, *Cont. Shelf Res.*, 60, 28–37,
736 doi:10.1016/j.csr.2013.04.019, 2013.
- 737 Langer, G., Geisen, M., Baumann, K.-H., Kläs, J., Riebesell, U., Thoms, S. and Young, J. R.: Species-specific
738 responses of calcifying algae to changing seawater carbonate chemistry, *Geochem. Geophys. Geosystems*,
739 7(9), 155–161, doi:10.1029/2005GC001227, 2006.
- 740 Langer, G., Gussone, N., Nehrke, G., Riebesell, U., Eisenhauer, A. and Thoms, S.: Calcium isotope
741 fractionation during coccolith formation in *Emiliana huxleyi*: Independence of growth and calcification rate,
742 *Geochem. Geophys. Geosystems*, 8(5), Q05007, doi:10.1029/2006GC001422, 2007.
- 743 Langer, G., Oetjen, K. and Brenneis, T.: Calcification of *Calcidiscus leptoporus* under nitrogen and
744 phosphorus limitation, *J. Exp. Mar. Biol. Ecol.*, 413, 131–137, doi:10.1016/j.jembe.2011.11.028, 2012.
- 745 Langer, G., Oetjen, K. and Brenneis, T.: Coccolithophores do not increase particulate carbon production
746 under nutrient limitation: A case study using *Emiliana huxleyi* (PML B92/11), *J. Exp. Mar. Biol. Ecol.*, 443,
747 155–161, doi:10.1016/j.jembe.2013.02.040, 2013.
- 748 LaRoche, J., Rost, B. and Engel, A.: Bioassays, batch culture and chemostat experimentation, Riebesell, U.,
749 Fabry, V.J., Hansson, L., Gattuso, J.-P. (Eds.), *Guide to Best Practices for Ocean Acidification Research and*
750 *Data Reporting*. Publications Office of the European Union., 2010.
- 751 Laws, E. A.: Evaluation of In Situ Phytoplankton Growth Rates: A Synthesis of Data from Varied Approaches,
752 *Annu. Rev. Mar. Sci.*, 5(1), 247–268, doi:10.1146/annurev-marine-121211-172258, 2013.
- 753 Leonardos, N. and Geider, R. J.: Elevated atmospheric carbon dioxide increases organic carbon fixation by
754 *Emiliana huxleyi* (Haptophyta), under nutrient-limited high-light conditions., *J. Phycol.*, 41(6), 1196–1203,
755 doi:10.1111/j.1529-8817.2005.00152.x, 2005.
- 756 Litchman, E., Klausmeier, C. A., Schofield, O. M. and Falkowski, P. G.: The role of functional traits and trade-
757 offs in structuring phytoplankton communities: scaling from cellular to ecosystem level, *Ecol. Lett.*, 10(12),
758 1170–1181, doi:10.1111/j.1461-0248.2007.01117.x, 2007.
- 759 Loisel, H., Nicolas, J.-M., Sciandra, A., Stramski, D. and Poteau, A.: Spectral dependency of optical
760 backscattering by marine particles from satellite remote sensing of the global ocean, *J. Geophys. Res.*,
761 111(C09024), doi:10.1029/2005JC003367, 2006.

- 762 Lomas, M. W. and Glibert, P. M.: Comparisons of Nitrate Uptake, Storage, and Reduction in Marine Diatoms
763 and Flagellates, *J. Phycol.*, 36(5), 903–913, doi:10.1046/j.1529-8817.2000.99029.x, 2000.
- 764 MacIntyre, H. L., Kana, T. M., Anning, T. and Geider, R. J.: Photoacclimation of Photosynthesis Irradiance
765 Response Curves and Photosynthetic Pigments in Microalgae and Cyanobacteria¹, *J. Phycol.*, 38(1), 17–38,
766 doi:10.1046/j.1529-8817.2002.00094.x, 2002.
- 767 Marañón, E., Cermeño, P., López-Sandoval, D. C., Rodríguez-Ramos, T., Sobrino, C., Huete-Ortega, M.,
768 Blanco, J. M. and Rodríguez, J.: Unimodal size scaling of phytoplankton growth and the size dependence of
769 nutrient uptake and use, *Ecol. Lett.*, 16(3), 371–379, doi:10.1111/ele.12052, 2013.
- 770 Monod, J.: The Growth of Bacterial Cultures., *Annual Review of Microbiology.*, 1949.
- 771 Morel, A., Gentili, B., Claustre, H., Babin, M., Bricaud, A., Ras, J. and Tièche, F.: Optical properties of the
772 “clearest” natural waters, *Limnol. Oceanogr.*, 52(1), 217–229, doi:10.4319/lo.2007.52.1.0217, 2007.
- 773 Moutin, T., Karl, D. M., Duhamel, S., Rimmelin, P., Raimbault, P., Van Mooy, B. A. S. and Claustre, H.:
774 Phosphate availability and the ultimate control of new nitrogen input by nitrogen fixation in the tropical
775 Pacific Ocean, *Biogeosciences*, 5(1), 95–109, doi:10.5194/bg-5-95-2008, 2008.
- 776 Müller, M. N., Antia, A. N. and LaRoche, J.: Influence of cell cycle phase on calcification in the
777 coccolithophore *Emiliana huxleyi*, *Limnol. Oceanogr.*, 53(2), 506–512, doi:10.4319/lo.2008.53.2.0506,
778 2008.
- 779 Müller, M. N., Beaufort, L., Bernard, O., Pedrotti, M. L., Talec, A. and Sciandra, A.: Influence of CO₂ and
780 nitrogen limitation on the coccolith volume of *Emiliana huxleyi* (Haptophyta), *Biogeosciences*, 9(10), 4155–
781 4167, doi:10.5194/bg-9-4155-2012, 2012.
- 782 Okada, H. and McIntyre, A.: Seasonal distribution of modern coccolithophores in the western North Atlantic
783 Ocean, *Mar. Biol.*, 54(4), 319–328, doi:10.1007/BF00395438, 1979.
- 784 Oviedo, A. M., Langer, G. and Ziveri, P.: Effect of phosphorus limitation on coccolith morphology and
785 element ratios in Mediterranean strains of the coccolithophore *Emiliana huxleyi*, *J. Exp. Mar. Biol. Ecol.*,
786 459, 105–113, 2014.
- 787 Paasche, E.: Reduced coccolith calcite production under light-limited growth: a comparative study of three
788 clones of *Emiliana huxleyi* (Prymnesiophyceae), *Phycologia*, 38(6), 508–516, doi:10.2216/i0031-8884-38-6-
789 508.1, 1999.
- 790 Paasche, E.: A review of the coccolithophorid *Emiliana huxleyi* (Prymnesiophyceae), with particular
791 reference to growth, coccolith formation, and calcification-photosynthesis interactions, *Phycologia*, 40(6),
792 503–529, doi:10.2216/i0031-8884-40-6-503.1, 2002.
- 793 Raimbault, P. and Garcia, N.: Evidence for efficient regenerated production and dinitrogen fixation in
794 nitrogen-deficient waters of the South Pacific Ocean: impact on new and export production estimates,
795 *Biogeosciences*, 5, 323–338, doi:10.5194/bg-5-323-2008, 2008.
- 796 Raimbault, P., Garcia, N. and Cerutti, F.: Distribution of inorganic and organic nutrients in the South Pacific
797 Ocean-evidence for long-term accumulation of organic matter in nitrogen-depleted waters, *Biogeosciences*,
798 5(2), 281–298, 2008.
- 799 Raven, J. A. and Crawford, K.: Environmental controls on coccolithophore calcification, *Mar Ecol Prog Ser*,
800 470, 137–166, doi:10.3354/meps09993, 2012.
- 801 Redfield, A. C.: The influence of organisms on the composition of sea-water, *The Sea*, 26–77, 1963.

802 Riegman, R., Stolte, W., Noordeloos, A. A. M. and Slezak, D.: Nutrient uptake and alkaline phosphatase (ec
803 3:1:3:1) activity of *Emiliana huxleyi* (PRYMNESIOPHYCEAE) during growth under N and P limitation in
804 continuous cultures, *J. Phycol.*, 36(1), 87–96, doi:10.1046/j.1529-8817.2000.99023.x, 2000.

805 Rokitta, S. D. and Rost, B.: Effects of CO₂ and their modulation by light in the life-cycle stages of the
806 coccolithophore *Emiliana huxleyi*, *Limnol. Oceanogr.*, 57(2), 607–618, 2012.

807 Rost, B., Zondervan, I. and Riebesell, U.: Light-dependent carbon isotope fractionation in the
808 coccolithophorid *Emiliana huxleyi*, 2002.

809 Roth, P. H.: Distribution of coccoliths in oceanic sediments, in *Coccolithophores*, pp. 199–218, Cambridge.,
810 1994.

811 Rouco, M., Branson, O., Lebrato, M. and Iglesias-Rodríguez, M. D.: The effect of nitrate and phosphate
812 availability on *Emiliana huxleyi* (NZEH) physiology under different CO₂ scenarios, *Front. Aquat. Microbiol.*,
813 4, 155, doi:10.3389/fmicb.2013.00155, 2013.

814 Sciandra, A., Harlay, J., Lefèvre, D., Leme, R., Rimmelin, P., Denis, M. and Gattuso, J.: Response of
815 coccolithophorid *Emiliana huxleyi* to elevated partial pressure of CO₂ under nitrogen limitation, *Mar. Ecol.*
816 *Prog. Ser.*, 261, 111–122, doi:10.3354/meps261111, 2003.

817 Selph, K. E., Landry, M. R., Taylor, A. G., Yang, E.-J., Measures, C. I., Yang, J., Stukel, M. R., Christensen, S.
818 and Bidigare, R. R.: Spatially-resolved taxon-specific phytoplankton production and grazing dynamics in
819 relation to iron distributions in the Equatorial Pacific between 110 and 140°W, *Deep Sea Res. Part II Top.*
820 *Stud. Oceanogr.*, 58(3–4), 358–377, doi:10.1016/j.dsr2.2010.08.014, 2011.

821 Shutler, J. D., Land, P. E., Brown, C. W., Findlay, H. S., Donlon, C. J., Medland, M., Snooke, R. and Blackford,
822 J. C.: Coccolithophore surface distributions in the North Atlantic and their modulation of the air-sea flux of
823 CO₂ from 10 years of satellite Earth observation data, *Biogeosciences*, 10(4), 2699–2709, doi:10.5194/bg-
824 10-2699-2013, 2013.

825 Terry, K. L.: Nitrate and phosphate uptake interactions in a marine Prymnesiophyte, *J. Phycol.*, 18(1), 79–86,
826 doi:10.1111/j.1529-8817.1982.tb03159.x, 1982.

827 Trimborn, S., Langer, G. and Rost, B.: Effect of varying calcium concentrations and light intensities on
828 calcification and photosynthesis in *Emiliana huxleyi*, *Limnol. Oceanogr.*, 52(5), 2285–2293,
829 doi:10.4319/lo.2007.52.5.2285, 2007.

830 Westbroek, P., Brown, C. W., Bleijswijk, J. van, Brownlee, C., Brummer, G. J., Conte, M., Egge, J., Fernández,
831 E., Jordan, R., Knappertsbusch, M., Stefels, J., Veldhuis, M., van der Wal, P. and Young, J.: A model system
832 approach to biological climate forcing. The example of *Emiliana huxleyi*, *Glob. Planet. Change*, 8(1–2), 27–
833 46, doi:10.1016/0921-8181(93)90061-R, 1993.

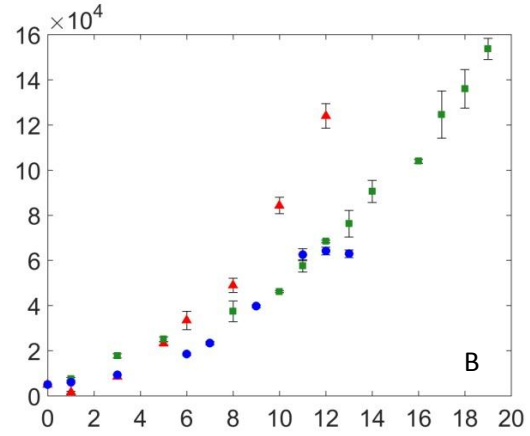
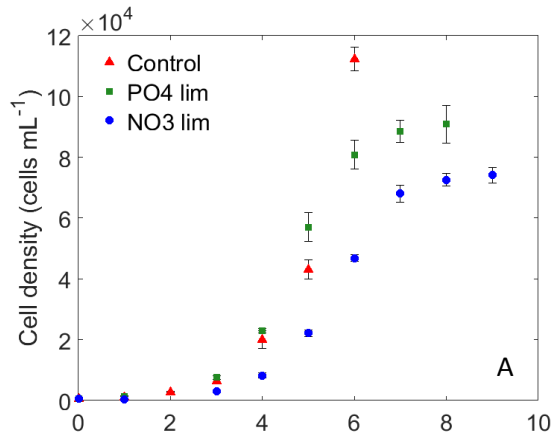
834 Winter, A., Henderiks, J., Beaufort, L., Rickaby, R. E. M. and Brown, C. W.: Poleward expansion of the
835 coccolithophore *Emiliana huxleyi*, *J. Plankton Res.*, 36(2), 316–325, doi:10.1093/plankt/fbt110, 2014.

836 Young, J. R., Poulton, A. J. and Tyrrell, T.: Morphology of *Emiliana huxleyi* coccoliths on the northwestern
837 European shelf—is there an influence of carbonate chemistry?, *Biogeosciences*, 11(17), 4771–4782,
838 doi:10.5194/bg-11-4771-2014, 2014.

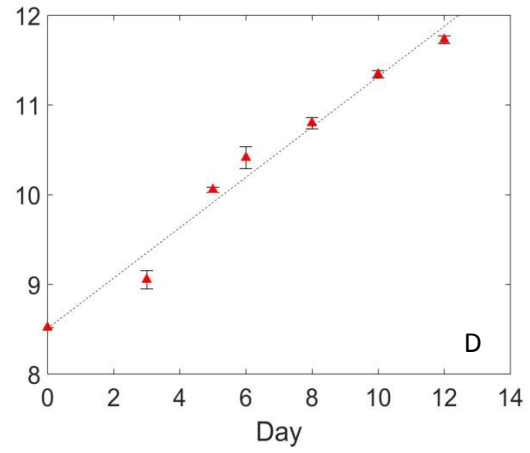
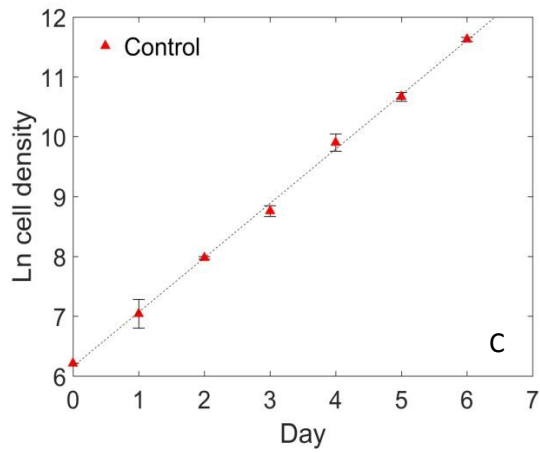
839 Zondervan, I.: The effects of light, macronutrients, trace metals and CO₂ on the production of calcium
840 carbonate and organic carbon in coccolithophores—A review, *Deep Sea Res. Part II Top. Stud. Oceanogr.*,
841 54(5–7), 521–537, doi:10.1016/j.dsr2.2006.12.004, 2007.

842

843



844



845

846 *Figure 1.* The evolution of cell density with time in culture experiments with *E. huxleyi* strain RCC911 (A:
847 high irradiance; B: low irradiance) and cell density on a logarithmic scale for nutrient-replete cultures (C:
848 high irradiance; D: low irradiance).

849

850

851

852

853

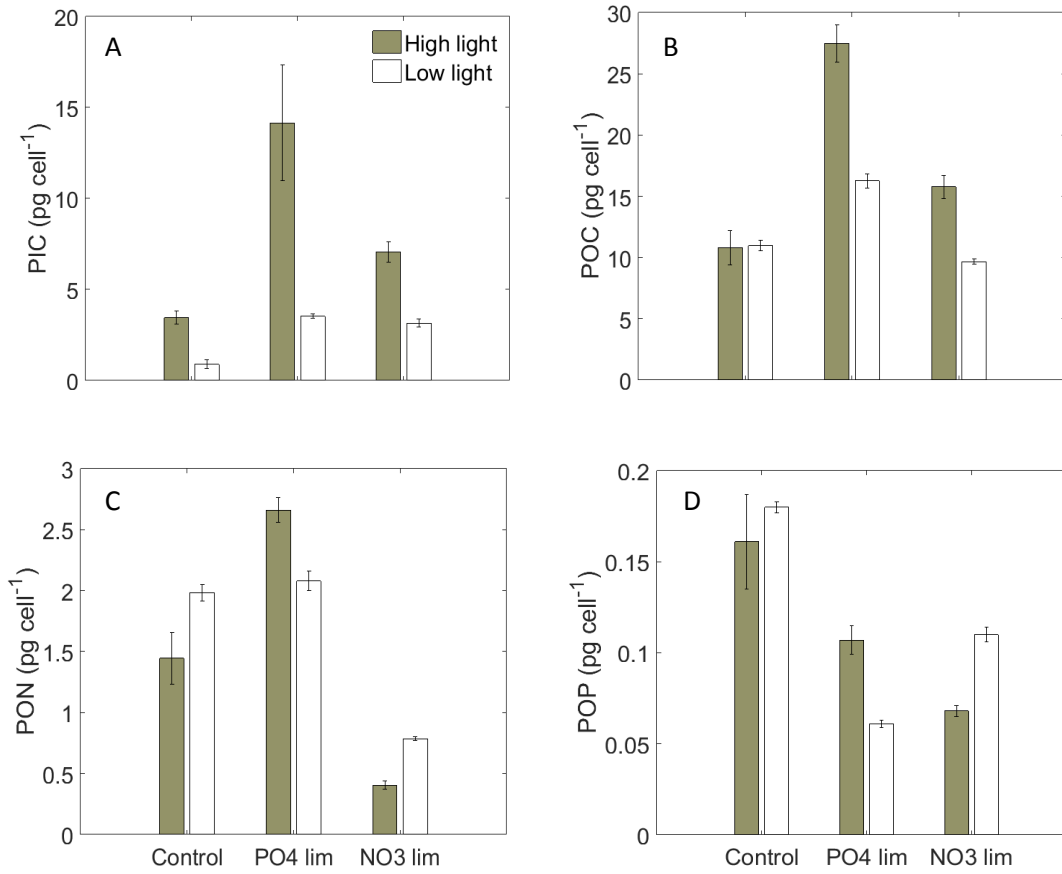
854

855

856

857

858



859

860

861 *Figure 2. Cellular PIC (A), POC (B), PON (C), POP (D) quotas.*

862

863

864

865

866

867

868

869

870

871

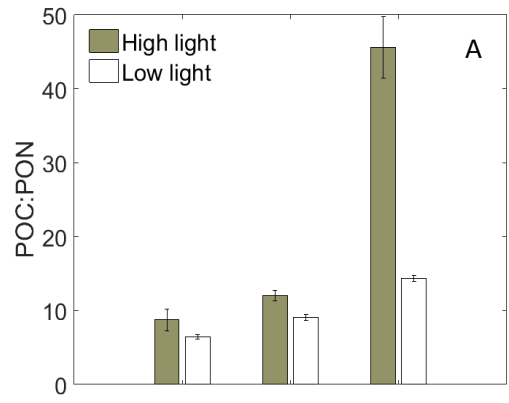
872

873

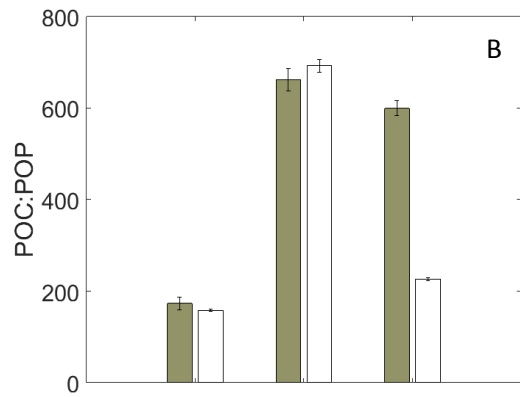
874

875

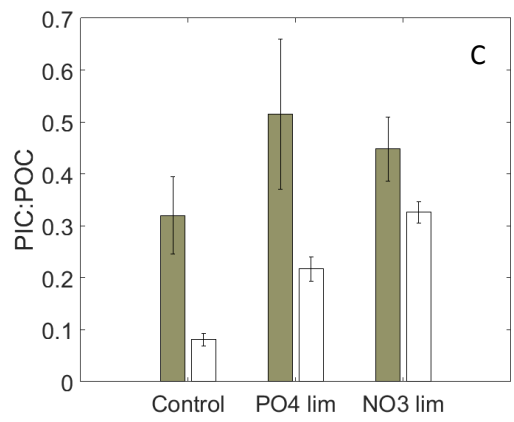
876



877



878



879

880 *Figure 3. Cellular POC:PON (A), POC:POP (B) and PIC:POC (C) ratios.*

881

882

883

884

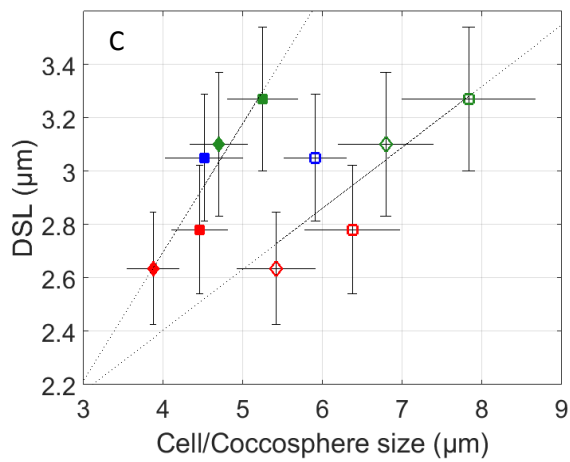
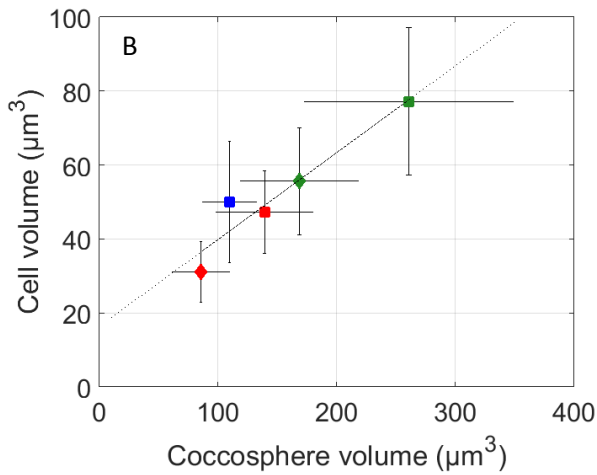
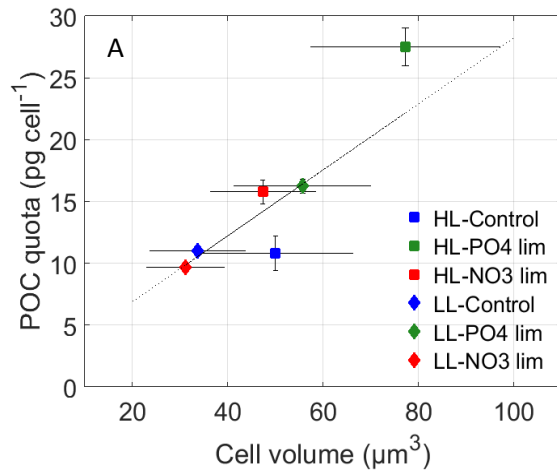
885

886

887

888

889



890

891

892

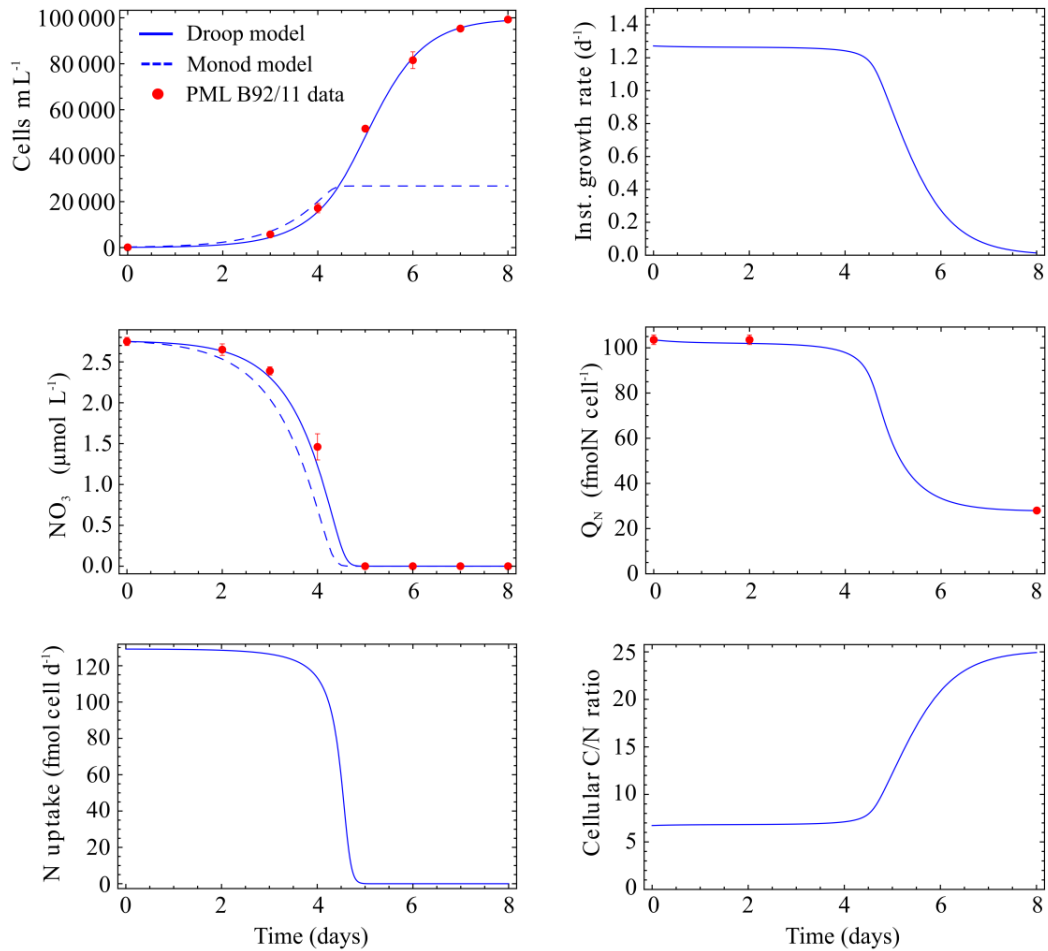
893 *Figure 4.* (A) POC quota versus cell volume; (B) Cell volume against coccosphere volume in high light (HL)
 894 and low light (LL) conditions; (C) Distal shield length (DSL) versus coccosphere and cell diameter. Solid
 895 symbols are cell size and open symbols are coccosphere size. Dotted line is the linear regression.

896

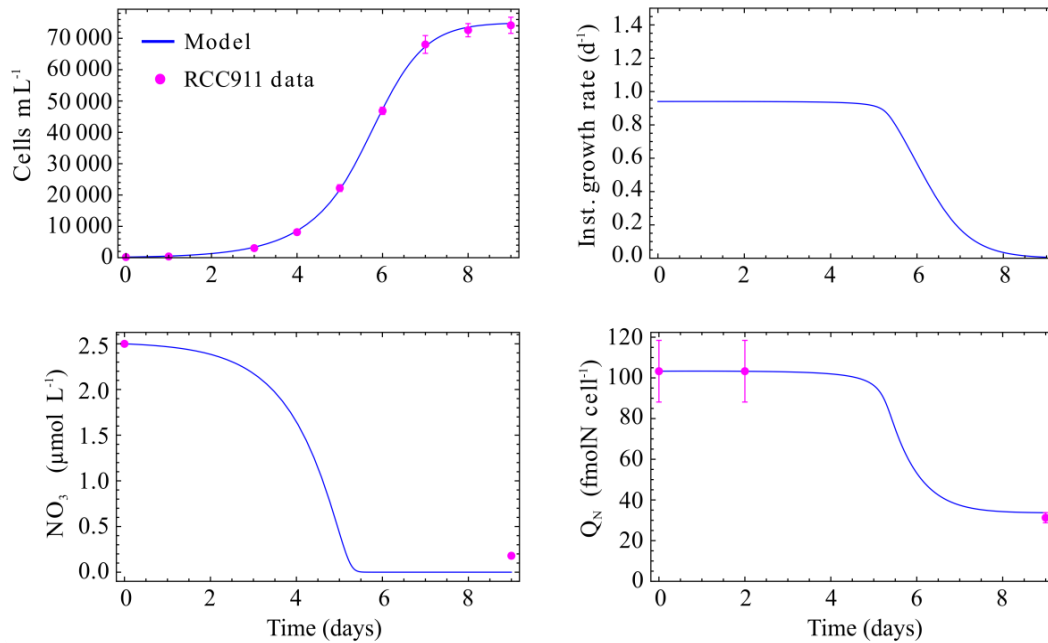
897

898

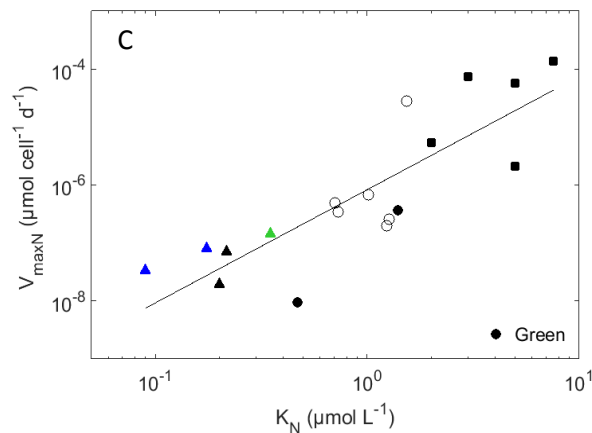
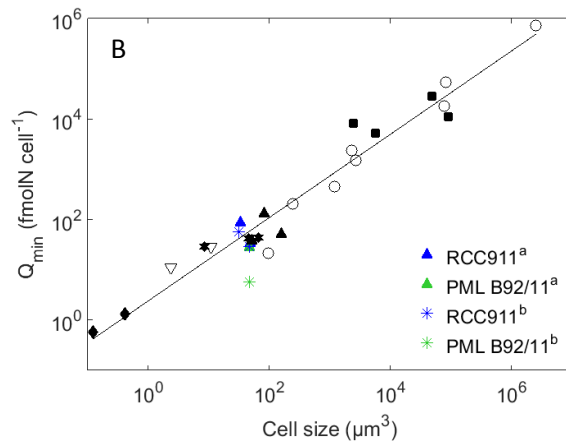
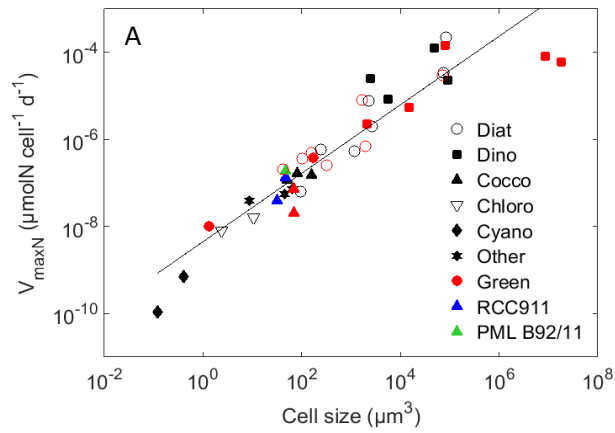
899



900
 901 *Figure 5. Model fitted to the data of the nitrate-limited cultures of Langer et al. (2013) (Inst =*
 902 *instantaneous).*
 903



904
 905 *Figure 6. Model fitted to the data of the nitrate-limited cultures of strain RCC911 in high light conditions.*



^a = model results; ^b = analysis results

906

907

908

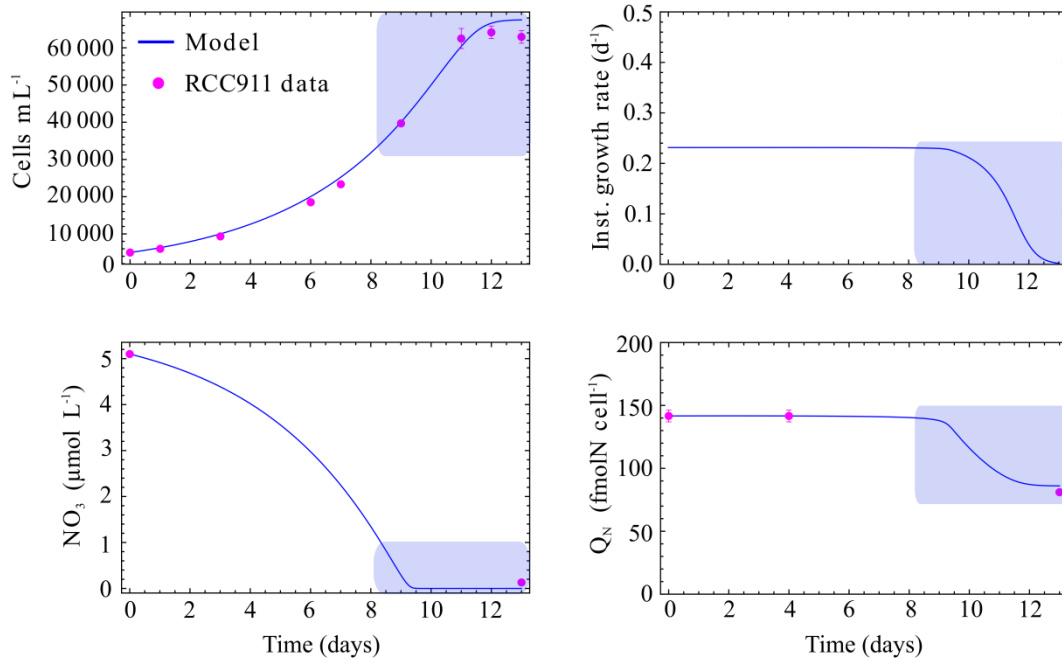
909

910

911 *Figure 7.* A) Maximum normalized surface uptake rate $V_{\max N}$ for nitrate versus the cell volume. Data from
 912 Marañón et al. (2013) in black, data from Litchman et al. (2007) in red and the Droop model output for the
 913 experiments presented in this work in blue and green depending of the strain; B) Minimum cellular quota
 914 Q_{\min} for nitrate versus the cell volume. Data of Marañón et al. (2013) and the results from the model and
 915 analysis of the present study; C) $V_{\max N}$ versus the half-saturation constant for nitrate uptake K_N . Data of
 916 Litchman et al. (2007) and results from the Droop model in nitrate-limited conditions.

917

918



919

920 *Figure 8.* Model fitted to the data of the nitrate limited cultures on RCC911 strain in low light. The shaded
 921 area corresponds to the equivalent nitrate concentration in the BIOSOPE ecological niche of
 922 coccolithophores at the GYR station (between 150 and 200 m depth).

923

924

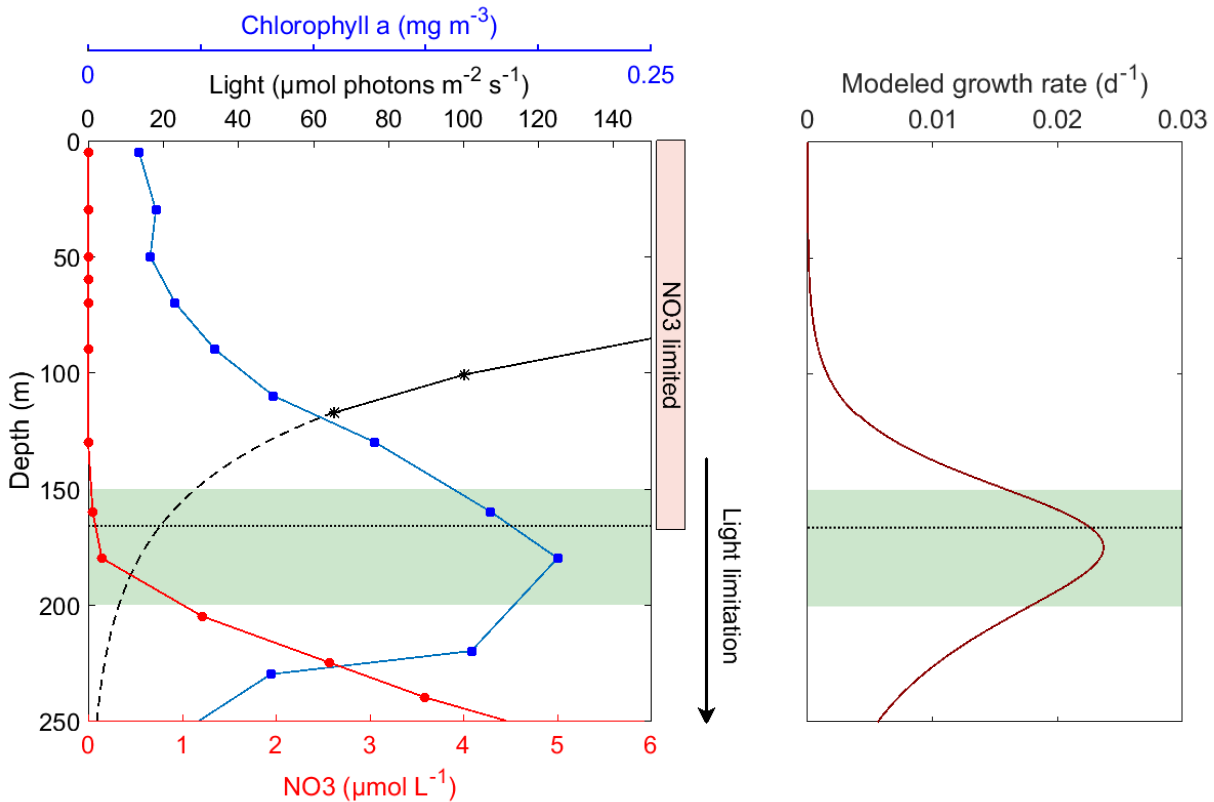
925

926

927

928

929



930

931 *Figure 9.* Left panel: In situ data (0 to 250 m) at the GYR station of the BIOSOPE transect (114.01° W, 26.06°
 932 S). Profiles of in situ measured chlorophyll a, PAR irradiance and nitrate concentration are shown. The
 933 dashed line represents an extrapolation of the irradiance between 117 m (last point measured) and 250 m
 934 considering a constant attenuation coefficient K_d ($K_d=0.025 \text{ m}^{-1}$ from Claustre et al., 2008) and a simple light
 935 calculation taken from MacIntyre et al. (2002). The dotted black line is the depth at which the K_N (0.09 μM)
 936 is observed. This depth also corresponds to the lower limit of nitrate limitation. Light limitation starts above
 937 the DCM and intensifies with depth. The green shaded area corresponds to the location of the maximum of
 938 coccosphere abundance taken from (Beaufort et al., 2008) between 120° W and 107° W. The right panel
 939 shows the growth rate of *E. huxleyi* with depth at the GYR station (calculated using Eq. A8).

940

941

942

943

944

945

946

947

948

949

950

951 *Table 1.* Growth rate, nutrient concentration, pH, DIC at the end of the experiments and shift in DIC
 952 compared with the initial DIC (averages from triplicate, n=3 for growth rates and nutrients analysis).

Sample	Growth rate ^a		NO ₃		PO ₄		pH		DIC		DIC shift
	<i>d</i> ⁻¹	<i>std</i>	$\mu\text{mol L}^{-1}$	<i>std</i>	$\mu\text{mol L}^{-1}$	<i>Std</i>	<i>std</i>	$\mu\text{mol kg}^{-1}$	<i>std</i>	%	
High light											
Control	0.91	0.03	67.92	1.98	3.95	0.12	8.13	0.01	2177	19.14	2.1
PO ₄ lim	0.00		80.88	0.35	0.01	0.00	8.21	0.01	1894	21.01	12.1
NO ₃ lim	0.00		0.18	0.03	5.74	0.00	8.14	0.00	2060	3.61	4.7
Low light											
Control	0.28	0.01	79.10	1.15	4.90	0.04	8.13	0.02	2161	7.55	4.1
PO ₄ lim	0.13	0.01	75.25	1.24	0.01	0.01	8.30	0.01	1956	8.33	13.2
NO ₃ lim	0.00		0.13	0.02	5.83	0.02	8.09	0.00	2139	4.16	39

953 ^a = cells are in exponential growth phase at the end of control experiments

954

955 *Table 2.* Cellular carbon, nitrogen and phosphorus quotas (averages from triplicate; n=6 for cellular
 956 quotas measurements).

Sample	PIC		POC		PON		POP		PIC:POC		POC:PON		POC:POP	
	pg cell^{-1}	<i>std</i>	pg cell^{-1}	<i>std</i>	pg cell^{-1}	<i>std</i>	pg cell^{-1}	<i>std</i>	<i>std</i>	<i>std</i>	<i>std</i>	<i>std</i>	<i>std</i>	<i>std</i>
High light														
Control	3.46	0.36	10.8	1.38	1.45	0.21	0.16	0.03	0.32	0.05	8.72	1.45	173	14.0
PO ₄ lim	14.16	3.19	27.49	1.53	2.66	0.10	0.11	0.01	0.52	0.12	12.05	0.70	661	24.3
NO ₃ lim	7.06	0.55	15.77	0.95	0.4	0.04	0.07	0.00	0.45	0.04	45.59	4.12	600	16.7
Low light														
Control	0.89	0.10	10.98	0.41	1.98	0.07	0.18	0.00	0.08	0.01	6.46	0.28	158	2.51
PO ₄ lim	3.53	0.25	16.25	0.56	2.08	0.08	0.06	0.00	0.22	0.017	9.11	0.41	693	13.4
NO ₃ lim	3.15	0.13	9.67	0.21	0.79	0.02	0.11	0.00	0.33	0.015	14.35	0.37	226	3.38

957

959 *Table 3.* Value of Q_R^{min} (which corresponds to the cellular PON (POP) at the end of the experiment:
 960 values measured and calculated) and the parameters obtained with the best-fit indicated for N and P
 961 limited experiment (high light: HL and low light: LL).

Strain	Light	Limitation	Q_R^{min}		V_{maxR} $\mu\text{mol cell}^{-1} \text{d}^{-1}$	Best-fit		
			Analysis fmol cell^{-1}	Calculation fmol cell^{-1}		K_R $\mu\text{mol L}^{-1}$	μ_{max} d^{-1}	KQ_R
PML B92/11		NO ₃	5.71	27.7	$1.46 \cdot 10^{-7}$	0.35	1.3	0.39
PML B92/11		PO ₄	0.645	2.04	$1.36 \cdot 10^{-8}$	0.051	1.57	0.98
RCC911	HL	NO ₃	28.57	31.28	$1.05 \cdot 10^{-7}$	0.205	1.01	0.25
RCC911	HL	PO ₄	3.464	5.931	$1.47 \cdot 10^{-8}$	0.35	1.2	0.9
RCC911	LL	NO ₃	56.14	78.99	$3.34 \cdot 10^{-8}$	0.09	0.2	0.3
RCC911	LL	PO ₄	1.968	2.875	$5.74 \cdot 10^{-10}$	0.275	0.52	0.47

